NASA TECHNICAL MEMORANDUM

NASA TM X-1548

NASA TM X-1548

PERFORMANCE OF A MULTITUBE SINGLE-PASS COUNTERFLOW NaK-COOLED MERCURY RANKINE-CYCLE CONDENSER

by Ronald H. Soeder, Joseph S. Curreri, and Robert P. Macosko

Lewis Research Center
Cleveland, Ohio

NATIONAL AERONAUTICS AND SPACE ADMINISTRATION • WASHINGTON, D. C. • APRIL 1968

NASA TM X-1548

PERFORMANCE OF A MULTITUBE SINGLE-PASS COUNTERFLOW NaK-COOLED MERCURY RANKINE-CYCLE CONDENSER

By Ronald H. Soeder, Joseph S. Curreri, and Robert P. Macosko

Lewis Research Center
Cleveland, Ohio

NATIONAL AERONAUTICS AND SPACE ADMINISTRATION

For sale by the Clearinghouse for Federal Scientific and Technical Information
Springfield, Virginia 22151 – CFSTI price $3.00

PERFORMANCE OF A MULTITUBE SINGLE-PASS COUNTERFLOW NaK-COOLED MERCURY RANKINE-CYCLE CONDENSER

by Ronald H. Soeder, Joseph S. Curreri, and Robert P. Macosko

Lewis Research Center

SUMMARY

Overall steady-state performance of a SNAP-8 condenser was mapped in a test facility simulating the SNAP-8 system. This condenser provided for a single pass of mercury in 73 tapered-diameter tubes cooled by counterflowing NaK (eutectic mixture of sodium and potassium) within a similarly tapered outer shell. The investigation was conducted for mercury flow rates from 4000 to 10 000 pounds mass per hour (0.5 to 1.3 kg/sec) and condenser NaK flow rates from 12 750 to 31 350 pounds mass per hour (1.6 to 4.0 kg/sec). The condensing lengths associated with the flow conditions ranged from 13 to 40 inches (0.3 to 1 m).

At the lower values of mercury and NaK flow rates, 4000 to 5000 pounds mass per hour (0.5 to 0.6 kg/sec) and 12 750 to 17 500 pounds mass per hour (1.6 to 2.2 kg/sec), respectively, there was close agreement between the values of condensing length indicated by a NaK stream temperature profile and an outer-shell temperature profile. The two profiles were measured 120° apart circumferentially. At the higher values of mercury and NaK flow rates, 7500 to 10 000 pounds mass per hour (1.0 to 1.3 kg/sec) and 29 000 to 31 350 pounds mass per hour (3.7 to 4.0 kg/sec), respectively, the condensing lengths indicated by the two separate temperature profiles did not agree. This condensing length disagreement indicated that a nonuniform distribution of NaK flow existed in the tube bundle.

The static-pressure drop of the mercury over the length of the condensing region varied, in general, between -1 and +1 psi ($\pm 6.9 \times 10^3$ N/m^2) for condensing lengths of 13 to 40 inches (0.3 to 1 m).

Average overall heat-transfer coefficients were calculated based on measured NaK stream temperatures. Corresponding saturated mercury vapor temperatures were obtained from the Lockhart-Martinelli correlation for an assumed liquid-to-vapor velocity ratio of 1.0. For the range of conditions investigated, the computed coefficients varied from 1980 to 3340 Btu per hour per square foot per $^{\circ}$F (1.1×10^4 to 1.9×10^4 W/(m^2)($^{\circ}$K)).

INTRODUCTION

One of the energy-conversion systems presently under investigation for electrical power generation in space is the SNAP-8 system. It is a nuclear Rankine cycle powerplant utilizing liquid metals as the working fluids. Mercury is vaporized in a boiler and then passes through a turbine, where some of its thermal energy is converted into mechanical energy. Turbine-exhaust vapor passes into a condenser wherein it is completely condensed and subcooled, and the waste heat of the cycle is transferred to NaK, the eutectic mixture of sodium and potassium. The waste heat is subsequently rejected to space by a radiator.

The SNAP-8 condenser is a counterflow heat exchanger which provides a single pass of mercury inside 73 tapered-diameter tubes within a tapered outer shell. In its operation, the condenser must provide (1) an exhaust pressure on the turbine low enough to allow the specified turbine power, (2) condenser-outlet pressure and subcooling that are high enough to provide adequate net positive suction head (NPSH) to the pump, and (3) liquid-mercury storage capacity.

The operating characteristics of a prototype SNAP-8 condenser were first evaluated and reported in reference 1. A further investigation of operating and heat-transfer characteristics was conducted in the Lewis SNAP-8 test facility. A second condenser, identical to that reported in reference 1, was used in the tests at Lewis, and the results of the Lewis studies are presented herein.

This investigation obtained overall condenser-performance data for variation in mercury flow rate, NaK flow rate, NaK inlet temperature, and mercury inventory. In particular, the study was concerned with the sensitivity of mercury-condenser-inlet pressure and mercury pressure drop to variations in NaK flow rate, NaK inlet temperature, and condensing length. Such information is pertinent to the satisfaction of the operating criteria regarding turbine-exhaust pressure and mercury pump NPSH. In addition to these studies, data obtained from parameter variations were used to compute average overall heat-transfer coefficient.

A supporting program of single-tube tests of mercury condensing had been previously conducted at Lewis. Overall heat-transfer characteristics of a single tapered tube identical to those in this condenser have been reported in references 2 and 3. Mercury-pressure-drop characteristics of a single tapered-diameter tube were investigated and reported in references 2, 4, and 5. Experimental data from these earlier single-tube tests are compared herein with the results of the multitube condenser tests. Also pressure drops were theoretically predicted from the Lockhart-Martinelli correlation and compared with the experimental data.

The ranges of independent variables employed in this investigation were as follows: mercury flow rate, 3200 to 10 000 pounds mass per hour (0.4 to 1.3 kg/sec); condensing

length, 8 to 48 inches (0.2 to 1.2 m); inlet quality, 0.80 to 1.00; NaK flow rate, 12 750 to 31 350 pound mass per hour (1.6 to 4.0 kg/sec); and NaK inlet temperature, 400° to 570° F (480 to 570° K). Because of facility limitations, design flow rates were not obtainable for direct comparison with data in reference 1.

APPARATUS

Test Facility

The test program was conducted in a test facility which simulated the basic SNAP-8 system. A simplified schematic diagram of the test loop showing the location of major components is shown in figure 1. In the primary loop, NaK, circulated by an electromagnetic pump, transferred heat from the electric heater to the mercury boiler. Liquid mercury flowing in the power loop was vaporized in the boiler and then passed through a turbine simulator consisting of two valves, two venturi meters, and a cooler. Mercury vapor flowed downward from the turbine simulator into the vertically mounted condenser. The liquid mercury was recirculated through the loop by a centrifugal pump.

The condensing mercury gave up its thermal energy to NaK which flowed vertically upward through the condenser, counter to the mercury flow. NaK flowed from the condenser through two heat exchangers where it was cooled by air flowing over the outside of finned tubes. The NaK flow then passed through an electromagnetic pump which returned the coolant to the condenser. Near the NaK condenser entrance, a three-way flow-control valve, on demand, allowed some of the NaK to bypass the condenser. This enabled condenser NaK flow rate to be varied with minimum operational changes.

The Condenser

A typical condenser cutaway assembly is illustrated in figure 2. As previously mentioned, the condenser was mounted vertically in the test facility. Mercury vapor flowed downward through 73 tapered-diameter tubes and the liquid collected in the lower plenum and the lower portion of the tubes. NaK entered at the bottom of the condenser in a toroidal plenum and was uniformly dispersed through holes drilled around the circumference of the condenser shell. NaK flowed vertically upward around the tubes cooling the mercury vapor and was collected in the outlet toroidal plenum. In order to distribute NaK uniformly over the outside of the mercury tapered tubes, a skirt (a sinusoidal-shaped transition section) was placed between the tubes and shell. This transition section extended from the NaK inlet to outlet plenums. NaK was discharged from the outlet plenum

through a transition section identical to that at the inlet.

The layout of the inlet and outlet mercury header plates for suspension of the condenser tubes is shown in figure 2. The tubes were installed in the tube bundle with their centerlines angled to achieve a constant NaK flow area along the tapered region. This maintained a constant NaK velocity in the critical-heat-transfer region of the condenser and allowed a more simplified analysis of average overall heat-transfer coefficient.

A single mercury condenser tube is also illustrated in figure 2. A 12.9-inch (0.3-m) straight section was attached to the bottom of the tapered tube in the subcooling region. The condenser was designed to establish a liquid-vapor interface in the tapered region of the tube at rated conditions of temperature, pressure and flow. The tube taper was for the purpose of maintaining high velocity throughout the condensing region and thus liquid-vapor-interface stability and stable condenser operation.

The tubes were fabricated from AISI 505 stainless steel (9 percent chromium-1 percent molybdenum). The outer condenser shell, the skirt, the NaK plenums, and NaK-inlet and -outlet transition pieces were constructed of AISI 410 stainless steel. The selection of AISI 505 and 410 steels was based on the similarity of thermal expansion coefficient in order to minimize the thermal stresses in the condenser.

INSTRUMENTATION

Temperature

Temperature-measuring instrumentation for the condenser tests consisted of thermocouples penetrating through the condenser shell and inner skirt into the NaK stream, and thermocouples on the inlet and outlet piping for the mercury and NaK. The thermocouple instrumentation on the condenser is shown in figure 3. All thermocouples were constructed of Instrument Society of America (ISA) standard calibration K (Chromel-Alumel) wires.

NaK inlet temperature was measured by averaging readings of three thermocouples spot-welded on the 7.66-inch (0.2-m) diameter NaK inlet manifold. The three thermocouples were equally spaced around the manifold circumference. NaK outlet temperature was determined by taking the average of six shell thermocouples placed on 60° centers on the 10.16-inch (0.3-m) diameter NaK outlet manifold. Twenty-three shell thermocouples (location Y on fig. 4) were spaced at 2-inch (5.1 cm) increments longitudinally along the shell, beginning at approximately $1\frac{3}{4}$ inch (4.5 cm) from the NaK outlet manifold. One hundred and eighty degrees circumferentially from the thermocouples, were located 22 shell thermocouples (location X on fig. 4), spaced at 2-inch (5.1 cm) intervals starting at approximately $2\frac{3}{4}$ inches (7.0 cm) from the NaK outlet manifold.

The mercury-inlet temperature was measured by a thermocouple embedded in the wall of a separate transition section, previously welded to the mercury condenser inlet header plate. Location of the mercury-vapor-inlet thermocouple was 16 inches (0.4 m) upstream of the NaK side of the tubes inlet header plate (see fig. 5). The mercury outlet temperature was measured by a thermocouple spot welded to the outlet pipe 2 inches (5.1 cm) below the mercury outlet plenum.

Welded tip, 1/8-inch (0.32 cm) diameter, sheath thermocouples were installed through the outer wall and flow skirt into the NaK flow of the condenser (see locations A and B on fig. 5). The thermocouples were set at a point 1/32 inch (0.08 cm) away from the innermost tube in the triangular pattern and brazed in place. Immersion thermocouples (location A) were located 30° circumferentially from the NaK outlet transition section. The first immersion thermocouple was set at 5.19 inches (0.13 m) from the inside face of the mercury inlet header plate. The next nine thermocouples were spaced at 3-inch (7.6 cm) intervals and the remaining eight thermocouples were set at 2-inch (5.1 cm) intervals. Immersion thermocouples (location B) were located 180° circumferentially from location A. The first thermocouple was set at 3.81 inches (9.7 cm) from the inside of the mercury inlet header plate. The following nine thermocouples were spaced at 3-inch (7.6 cm) increments. The distance between the tenth and eleventh immersion thermocouples was $2\frac{1}{2}$ inches (6.4 cm). The remaining seven thermocouples were spaced at 2-inch (5.1 cm) increments.

Pressure

Static pressures at mercury-inlet and -outlet plenums and NaK-inlet and -outlet manifolds were measured by inductive, slack-diaphragm, Bourdon tube pressure transducers. These transducers have the advantage of being calibrated at room temperature without displaying noticeable zero shift in calibration at elevated loop temperatures of 700° to 1000° F (645° to 810° R). Zero-shift is absent because the diaphragm of the unit was the only section of the transducer subjected to high temperatures. The main body of the pressure transducer consisted of Bourdon tube, mechanical linkage and inductance coil separated from the slack diaphragm by approximately 10 feet (3.1 m) of 1/8-inch (0.32 cm) capillary tubing.

Flow

NaK flow into the condenser was measured by an electromagnetic flowmeter. This flowmeter consisted of three parts: permanent magnet, flow tube, and electrodes. Liquid NaK flowed through the tube and produced an electromagnetic flow proportional to

volumetric flow rate. The temperature of the NaK was measured by a thermocouple located on the flow tube. This temperature was required to determine a value of NaK fluid density for converting measured volumetric flow into mass flow rate.

Liquid mercury flow was measured by a calibrated venturi flowmeter downstream of the pump. Mercury-inlet temperature and venturi flowmeter pressure drop were measured to calculate liquid mercury flow rate. Pressure drop from the venturi flowmeter inlet to throat was obtained from a 20 psi (1.4×10^5 N/m^2) differential pressure transducer. A pressure tap at the venturi flowmeter inlet and throat were connected to separate slack diaphragms. These two diaphragms were connected to a central diaphragm by 10 feet (3.1 m) of 1/8-inch (0.32 cm) capillary tubing. A mechanical linkage from the central diaphragm converted diaphragm movement into an electrical signal which was recorded as a pressure differential.

A complete description of all the instrumentation utilized in the SNAP-8 test facility is reported in reference 6.

Data Recording

All pressure and temperature data used for analyses were recorded on a central automatic digital data encoder (CADDE) whose function was to record data on demand from the control room. The only exception to this mode of data recording was the NaK shell temperature profile (location Y on fig. 5), which was displayed on a profile moniter.

PROCEDURE

Prior to a series of data runs, a complete calibration of absolute and differential pressure transducers was performed at room temperature in the test facility. The calibration consisted of applying several pressures of argon gas to the system. The measured electrical output was compared with a precision reference Bourdon gage. An additional step required in the calibration of the mercury differential-pressure transducer was that the low-pressure side of the unit was opened to atmospheric pressure before a selected range of pressures was applied to the mercury loop. The results obtained from the test facility calibration of both types of transducers coincided with the manufacturer's room-temperature calibrations. In the data analysis, a separate bench calibration at elevated temperature accounted for any zero shift in transducer calibration due to elevated temperature.

The venturi for measuring total mercury flow rate was water-calibrated and checked

against standard ASME fluid-meter specifications. Because of high system flow rates, it was not possible to calibrate the electromagnetic flowmeter which recorded NaK condenser flow rate. The manufacturer's standard calibration supplied with the unit was used.

The level of condenser cleanliness may affect the overall heat-transfer performance. Before installation in the facility, the NaK and mercury condenser passages were flushed with NA 500 (trichloroethane), followed by an oil-free argon purge. After the condenser was installed as part of the test facility, it was again flushed with NA 500. The formation of sodium and potassium oxides in the loops can cause plugging in the lines; therefore, an 8-hour hot NaK flush was executed at 700° to 800° F (645° to 700° K). The NaK was then allowed to flow into a dump tank to precipitate the oxides. If the oxide content was high (over 50 ppm), another hot flush was made, but if the level was satisfactory (under 20 ppm), data runs were started. A complete description of primary-loop, power-loop, and heat-rejection-loop cleanliness is reported in reference 7.

Condenser steady-state performance was obtained from a series of tests with the variables NaK flow rate, NaK inlet temperature, and mercury inventory. Each variable was changed while the other two were held constant. A test of each variable consisted of first establishing initial conditions and then incrementally changing the parameter to be investigated. Data were recorded at the start of each test and, after each incremental change, when the system reached steady-state conditions.

The initial test consisted of studying mercury-condenser-inlet pressure as a function of NaK flow rate. The NaK flow rate was varied from 14 500 to 29 500 pounds mass per hour (1.8 to 3.7 kg/sec) by controlling the NaK flow rate through the bypass line. This test was repeated for two mercury flow rates of 7580 and 6320 pounds mass per hour (1.0 and 0.8 kg/sec) at a NaK inlet temperature of approximately 480° F (520° K). Condenser NaK inlet temperature was held constant by controlling the air flow over the heat exchangers that cooled the NaK. The range of mercury-condenser-inlet pressure for both tests was from 6 to 20 psia (4.1×10^4 to 1.4×10^5 N/m^2).

Mercury-condenser-inlet pressure was investigated as a function of NaK inlet temperature for 7340 and 6350 pounds mass per hour (0.9 and 0.8 kg/sec). The condenser NaK inlet temperature was varied by altering the air flow over the radiators. Mercury-inlet pressure varied from approximately 4 to 19 psia (2.8×10^4 to 1.3×10^5 N/m^2).

Mercury-condenser-inlet pressure as a function of condensing length was studied by adding liquid mercury to the power loop in 10-pound (0.45-kg) increments between pump inlet and condenser outlet. Because no changes were made in power-loop operating conditions during the test, the mercury from each incremental injection accumulated in the condenser as liquid. This test was performed at a mercury flow of 7440 pounds mass per hour (0.9 kg/sec). The range of condensing lengths was from 40 to 20 inches (1.0 to 0.5 m).

METHOD OF ANALYSIS

Overall thermal conductance for the portion of the condenser tube upstream of the liquid-vapor interface is mathematically expressed as

$$\int_{l_1}^{l_c} U\pi D \, dl = -w_{NaK,c}\bar{c}_{p_{NaK}}\left[ln\left(\frac{T_{g,sat} - T_{NCO}}{T_g - T_{NaK}}\right) + \int_{l_1}^{l_c} \frac{\left(\frac{dT_g}{dl}\right)}{(T_g - T_{NaK})} \, dl\right] \quad \text{(B4)}$$

(symbols are defined in appendix A, and the equation is derived in appendix B). Selection of the length l_1 for the first 1-inch increment used in the calculation of overall conductance was based on visual inspection of mercury and NaK profiles for each condenser run.

In many instances, the value determined for condenser-inlet saturation temperature was nearly coincident with or less than the recorded NaK outlet temperature, the result being discrepancies in the calculated mercury temperature profiles and the measured NaK temperature profiles. Where ever the calculated mercury profile dipped below the NaK profile, or where the profiles were approximately coincident, all 1-inch (2.5 cm) increments comprising this section were disregarded in the calculation of $\overline{U}$. A resultant effective length l_{eff} was used in the heat-transfer calculations. A minimum of five satisfactory, adjacent 1-inch increments was arbitrarily selected as the criterion for use of a given condenser run in the overall-heat-transfer analysis.

The apparent mercury-to-NaK temperature disagreement could have been the result of a small error in mercury-inlet pressure measurement of approximately 1/2 psia (3.5×10^3 N/m^2). The mercury-condenser-inlet pressure range investigated in this study varied from 5 to 20 psia (3.5×10^4 to 1.4×10^5 N/m^2). An error in the pressure reading of 1/2 psia (3.5×10^3 N/m^2) would result in an error of 3° to 7° F (2° to 4° K) in saturated-mercury-vapor temperature at the condenser inlet.

The summation of incremental local conductances was divided by the summation of the incremental tube areas to give the average overall heat-transfer coefficient $\overline{U}$. The general mathematical notation to obtain $\overline{U}$ for a specific condenser run, starting at a length l_1 and terminating at an established condensing length l_c was expressed as

$$\overline{U} = \frac{\int_{\pi Dl_1}^{\pi Dl_c} U dA}{\int_{\pi Dl_1}^{\pi Dl_c} dA} \quad \text{(B6)}$$

A typical plot of the $\int UdA$ as a function of the $\int dA$ is illustrated in figure 6. The slope of the straight line is the average overall heat-transfer coefficient for the runs investigated.

Because the local mercury temperature was not acquired experimentally, it was assumed to be the local saturation temperature corresponding to a theoretical static-pressure profile. These profiles were calculated using the following technique from reference 4. Two-phase frictional pressure drop and the change due to momentum considerations were calculated at 1-inch (2.5-cm) increments starting at the inlet to the tube bundle. For the first increment, the sum of the two pressure changes was subtracted from the inlet static-pressure measurement to give the local theoretical static pressure at the beginning of the second 1-inch (2.5-cm) increment. The calculations were continued along the condensing length until the mercury interface was reached. The entrance pressure drop from the vapor inlet header to the condensing tubes was neglected because calculations, based on the contraction factor of a sharp-edged orifice, gave a maximum pressure difference of 1 percent.

The two-phase frictional pressure change was calculated from the Lockhart-Martinelli correlation (ref. 8). The momentum pressure change was calculated for an assumed liquid-to-vapor velocity ratio of 1.0. This assumption was based on the investigation of reference 4 which determined that the Lockhart-Martinelli correlation, with a liquid-to-vapor velocity between 0.5 to 1.0, agreed best with pressures measured in the first 75 percent of the vapor length. The general expression used to calculate local static-pressure drop for an assumed liquid-to-vapor velocity ratio of 1.0 is

$$\Delta P_s = \left[\Phi_g^2 \left(\frac{dP_g}{dL}\right)\right]_{(i+1,i)} \cdot \Delta L + \frac{w_{TM}}{g_c \bar{A}_t}\left(V_{g,i+1} - V_{g,i}\right) \qquad \text{(B31)}$$

The derivation of this equation appears in appendix B.

The physical properties of mercury vapor and liquid at saturated conditions were obtained from references 9 and 10. The thermodynamic properties of NaK were obtained from reference 9.

RESULTS AND DISCUSSION

Experimental data and calculated results are tabulated in tables I to III. Table I was used to present results illustrated in figures 7 to 9 and 15. Figures 6, 12, and 14 used information in table II, and figure 13 obtained information from table III. Results illustrated in figures 10 and 11 were obtained from tables I and II.

Effects of NaK Flow, NaK Inlet Temperature, and Mercury Inventory on Condensing Pressure

The effect of condensing pressure is illustrated in figure 7 for mercury flow rates of 6320 and 7580 pounds mass per hour (0.8 and 1.0 kg/sec). NaK inlet temperature was held constant at about 480° F (520° K). Although the condenser-design NaK flow rate of 40 000 pounds mass per hour (5.0 kg/sec) and the mercury design flow rate of 11 500 pounds mass per hour (1.5 kg/sec) were not achieved, an indication of the design-point condensing pressure can be obtained from figure 7 by consideration of the flow-rate ratio. The dashed line on figure 7 shows that the NaK-to-mercury condenser-design flow-rate ratio of 3.48 results in a mercury-vapor condenser-inlet static pressure of 9 psia (6.3×10^4 N/m^2). System design requirements dictate that the condenser-inlet pressure should not exceed a value of 14 psia (9.7×10^4 N/m^2) at the design point, otherwise turbine power is below the specified value. From figure 7, it can be determined that a reduction of about 20 percent in flow-rate ratio can be tolerated before the condenser-inlet pressure exceeds a value of 14 psia (9.7×10^4 N/m^2).

The effect of NaK inlet temperature on mercury condenser inlet pressure for two mercury flow rates of 7340 and 6350 pounds mass per hour (0.9 and 0.8 kg/sec) is shown in figure 8. The inlet pressure is very sensitive to condenser NaK inlet temperature. An increase in NaK inlet temperature of 1.25 times its initial value results in a pressure increase of 3.5 to 5 times its initial value.

Information obtained from a test indicating the effects of mercury inventory on condenser-inlet pressure is presented in figure 9. Forty pounds (18 kg) of liquid mercury, in 10-pound (4.5-kg) increments were added to the condenser inventory. Condensing length, to the nearest 1-inch (2.5-cm) increment, was determined from NaK temperature profiles obtained from immersion thermocouples on side A of the condenser. The range investigated was from 40 inches to 20 inches (1.0 to 0.5 m). No variation in mercury inlet pressure occurred for this range of condensing length. For shorter lengths, however, pressure is expected to increase rapidly with decreasing condensing length, as shown by the dashed line in figure 9. A thorough description of the theoretical shape of a curve of mercury-vapor condenser-inlet pressure as a function of condensing length is given in reference 11.

Single tapered condenser-tube studies by Albers and Namkoong (ref. 2) for condensing lengths of 20 inches (0.5 m) and longer, displayed a flat curve similar to that presented in figure 9. At condensing lengths less than 16 inches (0.4 m), these single-tube data indicated that mercury condenser inlet pressure became very sensitive to changes in mercury inventory. Reference 1 presented similar results of a pressure-sensitive region at condensing lengths less than 25 inches (0.6 m).

Pressure Drop

Although only overall pressure measurements were made, mercury-vapor static-pressure drop was determined by calculating a pressure at the vapor-liquid interface and subtracting this value from the inlet pressure measurement. The static pressure at the vapor-to-liquid interface was calculated from the measured outlet pressure as follows:

$$P_{g,\,int} = \left(P_{MCO} - L_{LIQ}\rho_l\right) = \left[P_{MCO} - (L_T - l_c)\,\rho_l\right] \tag{1}$$

The term L_t (total mercury vapor and liquid length) was the distance from the inside face of the mercury inlet header plate (start of condensing) to the point where the outlet mercury pressure was measured. The condensing length (l_c), used in equation (1) and plotted as the independent variable in figures 10 and 11 was obtained from a smooth curve drawn through NaK immersion-thermocouple temperature measurements (location A of the condenser). These NaK immersion-thermocouple profiles were drawn using shell temperatures as a guide.

The resulting experimental vapor-pressure-drop data are presented in figure 10 as a function of condensing length. This figure shows that, for the condensing lengths investigated (13 to 40 inches (0.3 to 1.0 m)), 75 percent of the pressure-drop data varied from -1 to +1 psi ($\pm 6.9\times10^3$ N/m^2). The range of mercury-flow rate for the pressure-drop data presented was from 4070 to 7440 pounds mass per hour (0.5 to 0.9 kg/sec) and for NaK flow rate from 13 000 to 29 000 pounds mass per hour (1.6 to 3.7 kg/sec). The absolute pressure of mercury vapor at the condenser inlet ranged from 5.5 to 19.5 psia (3.8×10^4 to 1.3×10^5 N/m^2).

Theoretical mercury-vapor static-pressure drops were calculated from the Lockhart-Martinelli correlation for a velocity ratio of $V_l/V_g = 1.0$. These theoretical values are compared with the experimental data in figure 11. For the theoretical calculation of mercury pressure drop, mercury and NaK flow rates and inlet and outlet pressures and temperatures encompassed the same ranges given for the experimental data. As shown in the figure, favorable agreement exists between the experimental and theoretical pressure drops. The best comparison occurred at medium condensing lengths of 20 to 27 inches (0.5 to 0.7 m), illustrated in figure 11(b). The experimental pressure-rise data varied between 0.4 to 1.0 psi (2.8×10^3 to 6.9×10^3 N/m^2), and the theoretical values varied between 0.6 to 0.7 psi (4.1×10^3 to 4.8×10^3 N/m^2) pressure rise. It was not possible to calculate theoretical two-phase static-pressure drop from the Lockhart-Martinelli correlation for all the test conditions in figure 10 because of the problem in temperature profiles discussed previously in the section METHOD OF ANALYSIS.

Temperature profiles. - A plot of three typical NaK-temperature profiles and the corresponding calculated mercury-vapor-temperature profiles are shown in figure 12. The NaK profiles were obtained from the immersion thermocouples at location A (fig. 5) and shell thermocouples. The NaK profile obtained from immersion thermocouples at location B (fig. 5) were discounted because 8 of the 18 thermocouples became defective during testing. The general trend indicated by shell temperature profiles was used as a guide in drawing a smooth curve through immersion-thermocouple temperature data. If the flat portion of the NaK profile originated within a given 1-inch (2.5-cm) increment, then condensing length was specified as the previous whole inch (2.5-cm) as measured from the inside face of the mercury inlet header plate. This is illustrated by the three NaK profiles in figure 12.

Use of NaK temperature profiles as a function of tube length to determine condensing length was justified by a heat-balance calculation performed between the mercury and NaK in the subcooled region of the condenser tube. The NaK temperature at the mercury interface $T_{NaK,int}$ was calculated from the heat-balance equation. For all runs, this calculated temperature was 2° to 5° F (1° to 3° K) greater than the temperature obtained at the condensing length selected from the NaK temperature profiles.

It can be seen from figure 12 that, in general, shell and immersion-thermocouple profiles are in close agreement, although the shell and immersion thermocouples are circumferentially separated by 120°. Close agreement between profiles suggests that the coolant flow was evenly distributed throughout the tube bundle. The levels of mercury and NaK flow rate varied from 3200 to 5000 pounds mass per hour (0.4 to 0.6 kg/sec) and 12 750 to 17 500 pounds mass per hour (1.6 to 2.2 kg/sec), respectively.

At higher mercury and NaK flow rates of 7500 to 10 000 pounds mass per hour (1.0 to 1.3 kg/sec) and 29 000 to 31 350 pounds mass per hour (3.7 to 4.0 kg/sec), respectively, the two profiles, 120° apart, gave different condensing lengths, indicating that the NaK flow was not uniformly distributed throughout the tube bundle. This is illustrated in figure 13 which shows the differences between the immersion-thermocouple (location A) and shell temperature profiles on the condenser (data run 63). This data run was obtained at a relatively high mercury flow rate of 8920 pounds mass per hour (1.1 kg/sec) and NaK flow rate of 30 550 pounds mass per hour (3.8 kg/sec). The third immersed thermocouple, located 11.2 inches (0.3 m) from the inlet, became inoperative during testing. Although this thermocouple defined a temperature on the NaK profile critical for medium condensing lengths, a curve was faired through the existing data. The shell-temperature measurements exhibited a gradual transition of temperature from the vapor to liquid regions (see fig. 13). This gradual transition results from a combination of NaK mixing and longitudinal conduction.

Heat-Transfer Coefficients

At low mercury and NaK flow rates, 3200 to 5000 pounds mass per hour (0.4 to 0.6 kg/sec) and 12 750 to 17 500 pounds mass per hour (1.6 to 2.2 kg/sec), respectively, the average overall heat-transfer coefficient (table II) varied from 1980 to 3020 Btu per hour per square foot per ^{o}F (1.1×10^{4} to 1.7×10^{4} $W/(m^{2})(^{o}K)$) with the arithmetical mean coefficient at 2440 Btu per hour per square foot per ^{o}F (1.4×10^{4} $W/(m^{2})(^{o}K)$). As shown in figure 14, no trend of $\overline{U}$ with condensing length could be established because of the scatter in the calculated points.

The higher values of mercury and NaK flow rates, 7500 to 10 000 pounds mass per hour (1.0 to 1.3 kg/sec) and 29 000 to 31 350 pounds mass per hour (3.7 to 4.0 kg/sec), respectively, yielded average overall heat-transfer coefficients of approximately 2230 to 3340 Btu per hour per square foot per ^{o}F (1.3×10^{4} to 1.9×10^{4} $W/(m^{2})(^{o}K)$) with the arithmetical mean coefficient at 2680 Btu per hour per square foot per ^{o}F (1.5×10^{4} $W/(m^{2})(^{o}K)$). These coefficients were based on NaK immersion-thermocouple temperature profiles (condenser, location A).

Comparison with Single-Tube Data

A comparison of temperature profiles from a single-tube test of reference 4 and from a test of this condenser is shown in figure 15. Comparable data from reference 4 and the SNAP-8 program were chosen. NaK temperature profiles were smooth curves drawn through NaK immersion-thermocouple temperatures. Corresponding saturated-mercury-vapor temperatures were obtained from the Lockhart-Martinelli correlation with a velocity ratio of $V_{l}/V_{g} = 1.0$. As shown by figure 15, the bulk of heat transfer for both condenser runs occurred from about the 9th to the 24th inch (0.2 to 0.6 m) of length from the inlet. In this region, average overall heat-transfer coefficients of 3100 and 2880 Btu per hour per square foot per ^{o}F (1.7×10^{4} to 1.6×10^{4} $W/(m^{2})(^{o}K)$) were calculated for the SNAP-8 condenser and the reference 4 condenser, respectively. The disagreement between these numbers is less than 10 percent.

For a number of runs with flow rates not far below the design value, arithmetical mean values for $\overline{U}$ were 20 percent lower for this condenser than for the single-tube condenser. The values obtained were 2680 and 3200 Btu per hour per square foot per ^{o}F (1.5×10^{4} to 1.8×10^{4} $W/(m^{2})(^{o}K)$) for this condenser and the single tube, respectively. In general, it is concluded that the heat-transfer results of this investigation are within 10 to 20 percent of the single-tube tests presented in references 3 and 4.

SUMMARY OF RESULTS

The results of an experimental investigation of the steady-state performance of the SNAP-8 condenser are summarized as follows:

1. For a constant condenser NaK inlet temperature of 495° F (530° K) and constant mercury and NaK flow rates of 7440 pounds mass per hour (0.9 kg/sec) and 29 000 pounds mass per hour (3.7 kg/sec), respectively, the mercury inlet pressure was insensitive to condensing lengths between 20 to 40 inches (0.5 to 1.0 m).

2. Approximately 75 percent of the pressure-drop data presented varied between -1 and +1 psi ($\pm 6.9 \times 10^3$ N/m^2) for condensing lengths from 13 to 40 inches (0.3 to 1.0 m). Favorable agreement with these results was obtained with calculations based on the Lockhart-Martinelli correlation with a velocity ratio of 1.0. These calculations gave a vapor pressure rise of from 0.1 to 0.7 psi (0.7×10^3 to 4.8×10^3 N/m^2) for approximately the same range of conditions as employed in obtaining the experimental data.

3. At mercury flow rates from 3200 to 10 000 pounds mass per hour (0.4 to 1.3 kg/sec) and condenser NaK flow rates from 12 750 to 31 350 pounds mass per hour (1.6 to 4.0 kg/sec), the average overall heat-transfer coefficients varied from 1980 to 3340 Btu per hour per square foot per °F (1.1×10^4 to 1.9×10^4 W/(m^2)(°K)). It was shown that, in general, the heat-transfer results of this investigation were in reasonable agreement with those of previous single-tube tests (ref. 4).

4. At low mercury and condenser NaK flow rates of 3200 to 5000 pounds mass per hour (0.4 to 0.6 kg/sec) and 12 750 to 17 500 pounds mass per hour (1.6 to 2.2 kg/sec), respectively, there was close agreement between the condensing length obtained from temperature profiles measured 120° apart, circumferentially. At high mercury flow rates (7500 to 10 000 lb mass/hr (1.0 to 1.3 kg/sec)) and NaK flow rates (29 000 to 31 350 lb mass/hr (3.7 to 4.0 kg/sec)), the condensing lengths obtained from the two profiles did not agree. This disagreement indicated that a nonuniform NaK flow distribution existed in the condenser tube bundle.

Lewis Research Center,
National Aeronautics and Space Administration,
Cleveland, Ohio, November 28, 1967,
701-04-00-02-22.

APPENDIX A

SYMBOLS

A	heat-transfer surface area, based on inside diameter of tube, ft^2; m^2
Ag	mercury vapor flow area, in^2; m^2
A_t	tube cross-sectional area, $in.^2$; m^2
$\bar{A}_t$	mean tube cross-sectional area for increment, $in.^2$; m^2
c_p	specific heat, Btu/(lb mass)(^oF); J/(kg)(^oK)
D	inside tube diameter, in.; m
f	friction factor, dimensionless
g_c	conversion factor, ft-lb mass/(lb force)(sec^2); (m)(kg)/(N)(sec^2)
h_{fg}	latent heat of vaporization, Btu/lb mass; J/kg
HTA	incremental heat-transfer area defined as $\int_{\pi D l_1}^{\pi D l_c} dA$, ft^2; m^2
L	length, in.; cm
l	distance from mercury inlet, in.; cm
l_1	distance from the mercury inlet to the first 1-inch (2.54-cm) increment selected for heat-transfer analysis, in.; m
l_c	condensing length, in.; m
l_{eff}	effective length for heat-transfer analysis, $(l_c - l_1)$, in.; m
L_{LIQ}	length of liquid mercury leg, in.; m
P	pressure, psia; N/m^2
Re	Reynolds number, dimensionless
T	temperature, ^oF; ^oK
U	overall heat-transfer coefficient, Btu/(hr)(ft^2)(^oF); W/(m^2)(^oK)
UdA	local conductance, Btu/(hr)(^oF); W/^oK
V	velocity, ft/sec; m/sec
v	specific volume, ft^3/lb mass; m^3/kg
W	mercury weight, lb force; N

w	flow rate, lb mass/hr; kg/sec
x	mercury quality, dimensionless
Δ	finite difference
ρ	density, lb mass/ft^3; kg/m^3
μ	dynamic viscosity, lb mass/(ft)(hr); N-sec/m^2
Φ_g	Lockhart-Martinelli parameter, dimensionless
χ	two-phase flow modulus $(\Delta P/\Delta L)_l / (\Delta P/\Delta L)_g$, dimensionless

Subscripts:

g	mercury vapor
g, int	mercury vapor at interface
g, sat	saturated mercury vapor
i	any section along the condenser tube
(i+1)	section 1 inch downstream from section i
IMM	immersion thermocouple temperature profile
IMMA	immersion thermocouples, location A on condenser
IMMB	immersion thermocouples, location B on condenser
in	inlet
int	interface
l	liquid mercury
l_1	distance from the mercury inlet to first 1-inch (2.54-cm) increment selected for heat-transfer analysis
l_c	condensing length
MCI	mercury condenser inlet
MCO	mercury condenser outlet
MOM	momentum
NaK	eutectic mixture of sodium-potassium
NaK, c	NaK side of the condenser
NCI	NaK condenser inlet
NCO	NaK condenser outlet
s	static

shell condenser shell

T total

TM total mercury

TPF two-phase friction

tt turbulent liquid, turbulent gas

vt viscous liquid, turbulent gas

Superscript:

$\bar{}$ average quantity

APPENDIX B

DERIVATION OF OVERALL HEAT-TRANSFER COEFFICIENT AND PRESSURE-DROP EQUATIONS

Average overall heat-transfer coefficient $\overline{U}$ is calculated on the condenser inlet. The following assumptions were made in evaluation of $\overline{U}$:

(1) Mercury saturation temperature was obtained from its corresponding calculated pressure. The two-phase friction contribution to pressure change was obtained from the Lockhart-Martinelli correlation. The momentum contribution to pressure change was predicted for a liquid-to-vapor velocity ratio of 1.0.

(2) The mechanism for energy exchange between mercury vapor and NaK was radial convective heat transfer plus conduction across the tube wall at a given cross section.

(3) The temperature of NaK measured by immersion thermocouples (condenser location A) at a given cross section was assumed to be the bulk temperature of the NaK.

(4) Losses due to radiative heat transfer from the condenser to the surroundings were assumed to be negligible because of insulation of the outer surface.

(5) The superheated vapor present at the condenser inlet had a negligible effect on radial convective heat transfer. The enthalpy content of the superheat was less than 3 percent of the latent heat of vaporization for all conditions investigated.

A heat balance at any longitudinal position l in the vapor section of the condenser tube results in

$$U\pi D\, dl \left(T_g - T_{NaK}\right) = -w_{NaK,c} \overline{c}_{p_{NaK}} dT_{NaK} \tag{B1}$$

Flow in the mercury direction was taken as positive (see fig. 16).

Rearrangement of equation (B1) and the addition and subtraction of dT_g from the right side of the equation yields

$$U\pi D\, dl = -w_{NaK,c} \overline{c}_{p_{NaK}} \left(\frac{dT_{NaK} - dT_g + dT_g}{T_g - T_{NaK}} \right) \tag{B2}$$

Integrating both sides of equation (B2) gives the following expression for overall unit conductance.

$$\int_{l_1}^{l_c} U\pi D\, dl = -w_{NaK,c} \overline{c}_{p_{NaK}} \left[\int_{l_1}^{l_c} \frac{-d(T_g - T_{NaK})}{(T_g - T_{NaK})} + \int_{l_1}^{l_c} \frac{\frac{dT_g}{dl}}{(T_g - T_{NaK})}\, dl \right] \tag{B3}$$

Equation (B3) is evaluated at the following boundary conditions:

$$T_g(l_1) = T_{g,\,sat} \quad \text{and} \quad T_{NaK}(l_1) = T_{NCO}$$

$$T_g(l_c) = T_{g,\,int} \quad \text{and} \quad T_{NaK}(l_c) = T_{NaK,\,int}$$

Evaluating equation (B3) at the specified boundary conditions

$$\int_{l_1}^{l_c} U\pi D\, dl = -w_{NaK,\,c}\,\bar{c}_{p_{NaK}} \left[l n \left(\frac{T_{g,\,sat} - T_{NCO}}{T_g - T_{NaK}} \right) + \int_{l_1}^{l_c} \frac{\left(\frac{dT_g}{dl} \right)}{(T_g - T_{NaK})}\, dl \right] \tag{B4}$$

Total heat-transfer area for the tapered tubes, from the inlet of the first 1-inch (2.5-cm) increment selected to the outlet of the last element coincident with condensing length l_c, may be expressed as

$$\int_{\pi D l_1}^{\pi D l_c} dA = \int_{l_1}^{l_c} 73\pi \left(\frac{D_{l_1} + D_{l_c}}{2.0} \right) dl \tag{B5}$$

The average overall heat-transfer coefficient is then expressed as the following general equation

$$\bar{U} = \frac{\int_{\pi D l_1}^{\pi D l_c} U\, dA}{\int_{\pi D l_1}^{\pi D l_c} dA} \tag{B6}$$

The local mercury saturation temperature was obtained from its corresponding local static pressure. These static pressures were obtained by calculating the static-pressure change for two-phase flow inside a tube. The calculational procedure was developed in reference 4. Neglecting the liquid droplet drag forces, the static-pressure change inside a tube is equal to the sum of the two-phase friction drop and pressure change due to momentum recovery.

$$\Delta P_s = \Delta P_{TPF} + \Delta P_{MOM} \tag{B7}$$

The Lockhart-Martinelli correlation (ref. 8) expressed two-phase frictional pressure gradient as a funcion of the parameter Φ_g and the frictional pressure gradient of the vapor. This pressure gradient is calculated on the basis of only vapor flow in the tube; therefore,

$$\frac{dP_{TPF}}{dL} = \Phi_g^2 \left(\frac{dP_g}{dL}\right) \tag{B8}$$

or, for a 1-inch (2.5-cm) increment,

$$\Delta P_{TPF} = \Phi_g^2 \left(\frac{dP_g}{dL}\right) \Delta L \tag{B9}$$

The parameter Φ_g is a function of the parameter χ for the Lockhart-Martinelli correlation. The value of χ depends on ficticious Reynolds numbers for the liquid and vapor phases, calculated on the basis that each component flowed alone inside the tube. Reynolds numbers less than 2000 were assumed to be viscous and those above 2000 were assumed to be in the turbulent regime. When calculated liquid and vapor Reynolds numbers were both greater than 2000, a turbulent-liquid - turbulent-vapor flow condition was assumed and χ was evaluated as follows:

$$\chi_{tt} = \left(\frac{1 - x}{x}\right)^{0.9} \left(\frac{v_l}{v_g}\right)^{0.5} \left(\frac{\mu_l}{\mu_g}\right)^{0.1} \tag{B10}$$

When an indicated viscous-liquid - turbulent-vapor flow condition existed (i.e., $Re_l < 2000$, $Re_g > 2000$) χ was determined from the following equation:

$$\chi_{vt} = \left(\frac{16.0}{0.046}\right)^{0.5} \left(\frac{v_l}{v_g}\right)^{0.5} \left(\frac{\mu_l}{\mu_g}\right)^{0.5} \left(\frac{1 - x}{x}\right)^{0.5} \left(\frac{1}{Re_g^{0.4}}\right) \tag{B11}$$

Mercury vapor quality x_i at 1-inch (2.5-cm) increments along the condensing length (from inlet to interface) was attained from a heat-balance ratio. The effects of saturated mercury vapor were accounted for, and quality at the vapor-liquid interface was assumed to be zero. This heat balance ratio is expressed as

$$\frac{w_{TM}\, h_{fg}(x_{in} - 0)}{w_{TM} h_{fg}(x_i - 0)} = \frac{w_{NaK,}\, c\bar{c}_{p,\, NaK}(T_{NCO} - T_{NaK,\, int})}{w_{NaK,}\, c\bar{c}_{p,\, NaK}\left(T_{NaK,\, i} - T_{NaK,\, int}\right)} \tag{B12}$$

Cancellation of similar terms plus the addition and subtraction of T_{NCO} to the denominator of the right hand side of equation (B12) yields the following results:

$$x_i = x_{in}\left(1 - \frac{T_{NCO} - T_{NaK,\, i}}{T_{NCO} - T_{NaK,\, int}}\right) \tag{B13}$$

The mercury condenser inlet quality x_{in} was calculated from the following heat balance between mercury and NaK

$$w_{TM}\left[x_{in}\bar{c}_{p_g}(T_{g,\, in} - T_{g,\, sat}) + x_{in}h_{fg} + \bar{c}_{p_l}(T_{g,\, sat} - T_{MCO})\right] = w_{NaK,}\, c\bar{c}_{p_{NaK}}(T_{NCO} - T_{NCI}) \tag{B14}$$

Neglecting the effects of superheated vapor and solving the above equation (B14) for mercury condenser inlet quality results in

$$x_{in} = -\frac{\left[\frac{w_{NaK,}\, c\bar{c}_{p_{NaK}}}{w_{TM}}\left(T_{NCO} - T_{NCI}\right) - \left(\bar{c}_{p_l}\; T_{g,\, sat} - T_{MCO}\right)\right]}{(h_{fg})} \tag{B15}$$

The vapor phase Reynolds numbers were always greater than 2000, and the frictional pressure gradient for this phase was evaluated by using the standard Fanning equation

$$\frac{dP_g}{dL} = \left(\frac{2.0 f V_g^2}{D v_g g_c}\right) \tag{B16}$$

The friction factor f of the Blasius form for turbulent flow in a smooth tube was assumed from reference 12

$$f = \frac{0.046}{Re_g^{0.2}} \tag{B17}$$

The vapor velocity at any section was determined from the continuity equation

$$V_{g,i} = \left(\frac{w_{TM} v_{g,i} x_i}{A_{g,i}} \right) \tag{B18}$$

where

$$w_{TM} = w_{l,i} + w_{g,i} \tag{B19}$$

and

$$A_{g,i} = \frac{A_{t,i}}{1.0 + \frac{v_{l,i}}{v_{g,i}} \left(\frac{1 - x_i}{x_i} \right)} \tag{B20}$$

Figure 17 illustrates the pressure change due to momentum consideration for a small incremental area. The result of inlet and outlet conditions yields

$$\Delta P_{MOM} = \frac{1}{g_c \bar{A}_t} \left[(w_g + dw_g)(V_g + dV_g) + (w_l + dw_l)(V_l + dV_l) - dw_g V'_g - dw'_l V'_l - w_g V_g - w_l V_l \right] \tag{B21}$$

where

$$\bar{A}_t = \frac{A_{t,i} + A_{t,i+1}}{2.0}$$

The term V'_g represents the velocity of the vapor condensed within the increment just before condensation takes place, and V'_l represents the velocity of the liquid droplets entrained into the vapor stream at the instant before the droplet is detached from the inner-tube wall. If $V'_g = V'_l = 0$, then equation (B21) may be rewritten as

$$\Delta P_{MOM} = \frac{1}{g_c \bar{A}_t} \left[(w_g + dw_g)(V_g + dV_g) + (w_l + dw_l)(V_l + dV_l - w_g V_g - w_l V_l \right] \tag{B22}$$

The vapor velocity V_g and the liquid velocity V_l were needed to evaluate equation (B22). The liquid velocity was obtained by assuming a liquid-to-vapor velocity ratio equal to 1.0.

Because steady flow existed throughout the incremental section, (fig. 17),

the total flow rate remained constant and any decrease in the vapor flow rate was offset by a corresponding increase in the liquid flow rate; therefore,

$$-dw_g = dw_l \tag{B23}$$

For a liquid-to-vapor velocity ratio of 1.0, it may be stated that

$$V_l = V_g \tag{B24}$$

and

$$dV_l = dV_g \tag{B25}$$

Substitution of equations (B23) to (B25) into equation (B22) yields the pressure change due to momentum considerations which is mathematically expressed as

$$\Delta P_{MOM} = \frac{1}{g_c \bar{A}_t} (w_g + dw_g)\left[dV_g + (w_l + dw_l)\right]dV_g \tag{B26}$$

Mercury vapor flow rate, at any increment along the condensing length can be expressed as a function of the total mercury flow rate and incremental quality as follows:

$$w_{g,i} = w_{TM}\, x_i \tag{B27}$$

Liquid-mercury flow rate, at any increment l of the condensing length l_c, may be determined from equation (B19).

The differentials dw_g and dV_g could be evaluated as finite differences from

$$\Delta w_g = w_{TM}(x_{i+1} - x_i) \tag{B28}$$

and

$$\Delta V_g = w_{TM} v_g \left(\frac{x_{i+1}}{A_{g,i+1}} - \frac{x_i}{A_{g,i}}\right) = \left(V_{g,i+1} - V_{g,i}\right) \tag{B29}$$

Substituting equations (B23), (B19), and (B29) into equation (B26) yields

$$\Delta P_{MOM} = \frac{w_{TM}}{g_c \bar{A}_t}\left(V_{g,i+1} - V_{g,i}\right) \quad \text{for } \frac{V_l}{V_g} = 1.0 \tag{B30}$$

The pressure change over a 1-inch (2.5-cm) increment using the Lockhart-Martinelli correlation and an assumed velocity ratio of 1.0 is

$$\Delta P_s = \left[\Phi_g^2 \left(\frac{dP_g}{dL}\right)\right]_{(i+1,\,i)} \cdot \Delta L + \frac{w_{TM}}{g_c \bar{A}_t} \left(V_{g,\,i+1} - V_{g,\,i}\right) \tag{B31}$$

REFERENCES

1. Kreeger, A. H.: Performance Map of the SNAP-8-1 Model Condenser, P/N 092500-1, S/N A-2, Rep. No. TM-4932-66-381 (NASA CR-72215), Aerojet-General Corp., Jan. 19, 1966.

2. Albers, James A.; and Namkoong, David, Jr.: An Experimental Study of The Condensing Characteristics of Mercury Vapor Flowing in Single Tubes. AIAA Specialists Conference on Rankine Space Power Systems. Vol. 1. AEC Rep. No. CONF-651026, Vol. 1, 1965, pp. 553-581.

3. Lottig, Roy A.; Vernon, Richard W.; and Kenney, William D.: Experimental Heat-Transfer Investigation of Nonwetting, Condensing Mercury Flow in Horizontal, Sodium-Potassium-Cooled Tubes. NASA TN D-3998, 1967.

4. Vernon, Richard W.; Lottig, Roy A.; and Kenney, William D.: Experimental Investigation of the Pressure Characteristics of Nonwetting, Condensing Flow of Mercury in a Sodium-Potassium-Cooled, Tapered Tube. NASA TN D-3691, 1966.

5. Albers, James A.; and Block, Henry B.: Experimental Pressure Drop Investigation of Wetting and Nonwetting Mercury Condensing in Uniformly Tapered Tubes. NASA TN D-3253, 1966.

6. Deyo, James N.; and Wintucky, William T.: Instrumentation of a SNAP-8 Simulator Facility. NASA TM X-1525, 1968.

7. Gorland, Sol H.; and Bilski, Raymond S.: Control of Contaminants in Liquid-Metal Systems. NASA TM X-1432, 1967.

8. Lockhart, R. W.; and Martinelli, R. C.: Proposed Correlation of Data for Isothermal Two-Phase, Two-Component Flow in Pipes. Chem. Eng. Progr., vol. 45, no. 1, Jan. 1949, pp. 39-48.

9. Weatherford, W. D., Jr.; Tyler, John C.; and Ku, P. M.: Properties of Inorganic Energy-Conversion and Heat-Transfer Fluids for Space Applications. (WADD TR-61-96), Southwest Research Institute, Nov. 1961.

10. Ross, D. P.: Thermodynamic Properties of Mercury. Rep. No. TM-777, Thompson-Ramo Woolridge, Inc., June 1957.

11. Packe, Donald R.; Schoenberg, Andrew A.; Jefferies, Kent S.; and Tew, Roy C.: Analysis of Condensing Pressure Control for SNAP-8 System. NASA TM X-1292, 1966.

12. McAdams, William H.: Heat Transmission. Third ed., McGraw-Hill Book Co., Inc., 1954.

TABLE I. - EXPERIMENTAL AND CALCULATED RESULTS FOR CONDENSER PERFORMANCE

Run	Total mercury flow rate, w_{TM}		Mercury condenser inlet pressure, P_{MCI}		Mercury condenser outlet pressure, P_{MCO}		Immersion thermocouple condensing length, $l_{c,IMMA}$		Mercury inlet quality, x_{in}	Inlet mercury vapor temperature, $T_{g,in}$		Saturated mercury vapor temperature, $T_{g,sat}$		Mercury condenser outlet temperature, T_{MCO}		Flow rate on NaK side of condenser, $w_{NaK,c}$		NaK condenser outlet temperature, T_{NCO}		NaK condenser inlet temperature, T_{NCI}		Mercury weight, W_M	
	lb mass/hr	kg/sec	psia	N/m^2	psia	N/m^2	in.	cm		^oF	^oK	^oF	^oK	^oF	^oK	lb mass/hr	kg/sec	^oF	^oK	^oF	^oK	lb force	N
1	7.55×10^3	0.95	8.0	5.5×10^4	18.2	12.5×10^4	37	94	0.83	625	603	617	598	479	521	29.37×10^3	3.70	615	596	478	521	--	---
2	7.52	.95	10.5	7.2	20.9	14.4	36	92	.87	649	616	642	612	480	522	24.70	3.11	644	613	478	521	--	---
3	7.62	.96	14.7	10.1	19.6	13.5	46	117	.85	680	633	676	630	484	524	20.98	2.65	677	631	482	523	--	---
4	7.62	.96	17.8	12.3	22.0	15.1	47	119	.85	698	644	695	641	485	524	19.34	2.45	696	636	483	524	--	---
5	7.61	.96	20.7	14.2	24.4	16.8	48	122	.83	714	652	711	650	486	525	17.56	2.21	713	651	484	524	--	---
6	6.29	.79	6.2	4.3	21.1	14.5	28	71	.85	603	591	594	586	481	522	29.65	3.74	592	585	480	522	--	---
7	6.33	.80	8.4	5.8	22.9	15.8	29	74	.82	627	604	621	600	484	524	23.38	2.95	623	601	484	524	--	---
8	6.35	.80	11.5	7.9	25.5	17.6	29	74	.84	657	619	651	616	485	524	19.47	2.45	654	618	483	524	--	---
9	6.31	.79	15.0	10.3	28.8	19.8	29	74	.80	681	634	678	631	483	523	16.21	2.04	679	631	482	523	--	---
10	6.32	.80	20.5	14.1	33.2	22.9	32	81	.83	713	653	710	649	483	523	14.49	1.83	713	651	482	523	--	---
11	5.20	.66	5.6	3.9	20.3	14.0	32	81	.98	706	647	584	579	481	522	29.82	3.76	587	581	479	521	--	---
12	5.29	.67	10.9	7.5	23.1	15.9	34	86	.98	727	658	645	613	489	526	20.18	2.57	651	616	489	527	--	---
13	5.34	.67	14.6	10.1	26.3	18.1	↓	↓	.96	736	664	675	629	489	↓	17.18	2.17	678	631	488	526	--	---
14	5.25	.66	17.7	12.2	29.4	20.2	↓	↓	.98	743	669	695	641	489	↓	15.49	1.95	698	643	488	526	--	---
15	5.34	.67	20.8	14.3	32.1	22.1	↓	↓	.96	749	672	712	651	488	↓	14.44	1.82	715	652	488	526	--	---
16	7.46	.94	11.8	8.1	21.5	14.8	40	102	.97	747	670	653	617	496	531	29.19	3.68	654	618	495	530	0	0
17	7.45	.94	11.9	8.2	24.0	16.5	34	86	.99	742	668	655	618	496	531	28.96	3.65	656	619	494	529	10	45
18	7.32	.92	11.2	7.7	26.0	17.9	29	74	.99	729	660	648	613	491	548	28.91	3.64	649	615	490	527	20	90
19	7.45	.94	12.2	8.4	29.2	20.1	24	61	.99	728	659	657	619	499	532	28.98	3.65	655	618	498	531	30	130
20	7.50	.95	12.1	8.3	31.3	21.6	20	51	.98	744	669	656	618	496	531	29.16	3.67	653	617	494	529	40	180
21	7.37	.93	4.4	3.0	17.7	12.2	38	97	.99	750	672	565	569	402	479	29.15	3.67	561	566	400	477	--	---
22	7.32	.92	5.5	3.8	18.7	12.9	36	91	.97	769	682	584	580	426	492	29.19	3.67	581	578	425	491	--	---
23	7.30	↓	7.1	4.9	20.2	13.9	34	86	.97	786	691	606	591	450	505	29.26	3.69	605	591	449	504	--	---
24	7.32	↓	9.3	6.4	22.1	15.2	34	86	.97	805	702	631	606	476	520	28.90	3.64	631	606	474	518	--	---
25	7.31	↓	11.6	8.0	23.7	16.3	34	86	.98	805	702	651	616	496	531	29.15	3.67	652	616	495	530	--	---
26	7.35	.93	15.4	10.6	26.7	18.4	35	89	.98	820	711	681	634	523	546	28.73	3.62	682	634	522	545	--	---
27	7.39	.93	19.4	13.4	30.3	20.9	36	91	.99	825	716	704	646	546	558	28.65	3.61	706	646	544	557	--	---
28	6.34	.80	5.6	3.9	21.8	15.0	27	69	.96	718	654	585	580	450	505	28.81	3.63	584	579	450	505	--	---
29	6.39	.81	7.4	5.1	22.4	15.4	29	74	.97	722	657	610	594	477	520	29.08	3.66	611	595	476	520	--	---
30	6.35	.80	10.0	6.9	24.3	16.8	29	74	.99	731	661	637	609	504	535	28.97	3.65	639	609	503	534	--	---
31	6.34	↓	12.6	8.7	26.3	18.1	31	79	.98	792	696	660	621	526	547	28.75	3.62	663	623	525	546	--	---
32	6.33	↓	15.9	11.0	28.2	19.4	33	84	.99	793	697	684	636	550	550	28.72	3.62	636	686	548	558	--	---
33	6.35	↓	19.0	13.0	31.6	21.8	32	81	.98	834	719	702	645	569	560	28.91	3.64	704	646	567	569	--	---

TABLE II. - EXPERIMENTAL AND CALCULATED RESULTS FOR LOW MERCURY FLOW RATES

Run	Total mercury flow rate, w_{TM}		Mercury condenser inlet pressure, P_{MCI}		Mercury condenser outlet pressure, P_{MCO}		Immersion thermocouple condensing length, $l_{c,IMMA}$		Effective length for heat-transfer analysis, $l_{c,IMMA\ eff}$		Mercury quality at inlet, x_{in}	Inlet mercury vapor temperature, $T_{g,in}$	
	lb mass/hr	kg/sec	psia	N/m^2	psia	N/m^2	in.	cm	in.	cm		^oF	^oK
34	3.17×10^3	0.40	10.0	6.9×10^4	29.7	20.5×10^4	8	20	7	18	0.85	643	612
35	3.69	.46	11.3	7.8	30.5	21.0	9	23	8	20	.93	654	618
36	4.55	.57	11.2	7.7	30.2	20.8	11	28	6	15	.88	653	617
37	4.94	.62	11.5	7.9	32.6	22.5	13	33	6	15	.97	660	621
38	4.93		11.3	7.8	32.5	22.4			6	15	.94	661	622
39	4.92		11.3	7.8	33.0	22.7			8	20	.96	662	623
40	4.91		10.9	7.5	32.1	22.1			6	15	.95	659	620
41	4.91		10.8	7.4	31.9	22.0					.95	657	619
42	4.91		10.8	7.4	31.4	21.6	14	36			.93	654	618
43	4.94		11.4	7.9	31.7	21.8	14	36			.94	660	621
44	4.94		11.2	7.7	31.5	21.7	15	38			.95	660	621
45	4.97	.63	11.5	7.9	32.0	22.0	14	36	7	18	.94	659	620
46	4.94	.62	11.2	7.7	30.7	21.2	16	41	6	15	.98	660	621
47	4.94		11.3	7.8	30.8	21.2	17	43	7	18	.98	661	622
48	4.94		11.4	7.9	30.6	21.1	17	43			.92	662	623
49	4.91		11.1	7.6	28.5	19.6	20	51			.94	660	621
50	4.91		11.0	7.6	28.6	19.7					.95	659	620
51	4.10	.52	15.8	10.9	32.5	22.4			8	20	.97	708	648
52	4.09		15.8	10.9	32.3	22.2			8	20	.98	707	647
53	4.09		16.1	11.1	32.7	22.5			10	25	.98	710	650
54	4.10		16.2	11.2	32.6	22.5			9	23	.97	711	651
55	4.10		16.0	11.0	32.6	22.5			10	25	.98	711	651
56	4.08	.51	16.1	11.1	32.5	22.4			8	20	.96	712	652
57	4.06		15.9	11.0	32.4	22.3					.99	715	653
58	4.07		15.9	11.0	32.5	22.4					.97	716	653
59	4.03		15.3	11.5	32.0	22.0					.97	717	654
60	4.03		15.3	11.5	32.0	22.0			9	23	1.00	716	653

TABLE II. - Concluded. EXPERIMENTAL AND CALCULATED RESULTS FOR LOW MERCURY FLOW RATES

Run	Saturated mercury vapor temperature, $T_{g, sat}$		Mercury condenser outlet temperature, T_{MCO}		Flow rate on NaK side of condenser, $w_{NaK, c}$		NaK condenser outlet temperature, T_{NCO}		NaK condenser inlet temperature, T_{NCI}		Overall heat-transfer coefficient, $\overline{U}$		Incremental heat-transfer area, HTA	
					lb mass/hr	kg/sec					Btu/(hr)(ft^2)(^oF)	W/(m^2)(^oK)	ft^2	m^2
	^oF	^oK	^oF	^oK			^oF	^oK	^oF	^oK				
34	637	609	519	544	14.47×10^3	1.82	637	609	522	546	2600	1.48×10^4	4.56	0.42
35	649	616	525	547	16.12	2.03	648	615	516	542	2560	1.45	5.17	.48
36	648	615	472	517	13.49	1.70	650	617	464	513	2720	1.54	3.70	.34
37	651	617	424	491	13.09	1.65	654	619	423	491	2280	1.29	3.57	.33
38	649	616	421	489	12.75	1.61	652	618	421	489	1980	1.12	3.57	.33
39	649	616	422	490	13.03	1.64	651	617	421		2320	1.32	4.85	.45
40	646	614	421	489	12.91	1.63	650	617	421		2040	1.16	3.57	.33
41	645	613	422	490	12.83	1.62	648	615	420		2370	1.34	3.57	
42	645	613	424	491	12.72	1.60	650	617	422	490	2410	1.37	3.51	
43	650	617	424	491	12.83	1.62	653	618	423	491	2500	1.42	3.51	
44	648	615	423	491	12.99	1.64	651	617	423	491	2420	1.37	3.45	.32
45	651	617	426	492	12.88	1.62	653	618	425	492	2410	1.37	4.13	.38
46	648	615	426	492	13.54	1.71	652	618	426		2430	1.38	3.39	.32
47	649	616	426	492	13.43	1.69	652	618	425		2300	1.30	3.92	.36
48	650	617	424	491	12.62	1.59	654	619	426		2270	1.29	3.92	.36
49	647	615	425	492	12.99	1.64	651	617	425		2810	1.60	3.70	.34
50	646	614	426	492	13.11	1.65	651	617	425		3020	1.71	3.70	.34
51	683	635	545	558	17.30	2.18	684	635	544	558	2420	1.37	4.27	.40
52	683	635	543	557	17.31	2.18	685	636	543	557	2400	1.36	4.27	.40
53	685	636	543	557	17.45	2.20	685	636	544	558	2580	1.46	5.44	.51
54	685	636	546	559	17.30	2.18	687	637	544	558	2540	1.44	4.85	.45
55	684	636	544	558	17.36	2.18	686	637	543	557	2410	1.37	5.44	.51
56	685	636	544	558	17.26	2.17	686	637	544	558	2660	1.51	4.27	.40
57	683	635	543	557	17.12	2.16	685	636	541	556	2430	1.38		
58	684	636	544	558	17.28	2.18	686	637	543	557	2420	1.37		
59	680	633	541	556	17.37	2.19	682	634	541	556	2240	1.27		
60	680	633	542	557	17.45	2.20	682	634	541	556	2290	1.30	4.85	.45

TABLE III. - EXPERIMENTAL AND CALCULATED RESULTS FOR MEDIUM AND HIGH MERCURY FLOW RATES

Run	Total mercury flow rate, w_{TM}		Mercury condenser inlet pressure, P_{MCI}		Mercury condenser outlet pressure, P_{MCO}		Mercury quality at inlet, x_{in}	Interface mercury vapor temperature, $T_{g,in}$		Saturated mercury vapor temperature, $T_{g,sat}$		Mercury condenser outlet temperature, T_{MCO}		Flow rate on NaK side of condenser, $w_{NaK,c}$		NaK condenser outlet temperature, T_{NCO}	
	lb mass/hr	kg/sec	psia	N/m^2	psia	N/m^2		^oF	^oK	^oF	^oK	^oF	^oK	lb mass/hr	kg/sec	^oF	^oK
19	7.45×10^3	0.94	12.2	8.4×10^4	29.2	20.1×10^4	0.99	728	659	657	620	499	532	28.98×10^3	3.64	655	619
61	7.45	.94	12.3	8.5	29.4	20.2	.99	729	660	658	620	500	533	29.12	3.67	655	619
20	7.50	.95	12.1	8.3	31.3	21.6	.98	744	668	656	619	496	531	29.16	3.67	653	618
62	7.48	.94	12.0	8.3	31.1	21.4	.97	743	668	655	619	494	529	29.03	3.66	650	616
63	8.92	1.12	10.3	7.1	20.0	13.8	.97	792	695	640	611	452	506	30.55	3.86	633	607
64	9.44	1.19	9.2	6.3	17.1	11.8	.99	780	688	630	605	431	495	30.92	3.89	623	601
65	9.38	1.18	9.2	6.3	17.2	11.9	.99	782	689	630	605	429	493	30.59	3.86	624	602
66	9.77	1.23	11.1	7.7	24.0	16.6	.99	803	700	647	614	438	498	31.20	3.93	647	614
67	10.04	1.26	12.2	7.8	23.0	15.9	1.00	809	704	656	619	444	502	31.35	3.96	650	616

Run	NaK condenser inlet temperature, T_{NCI}		Shell								Immersion thermocouple							
			Condensing length, l_c		Effective condensing length for heat transfer analysis, l_{eff}		Overall heat-transfer coefficient, $\overline{U}$		Incremental heat-transfer area, HTA		Condensing length, l_c		Effective condensing length for heat-transfer analysis, l_{eff}		Overall heat-transfer coefficient, $\overline{U}$		Incremental heat-transfer area, HTA	
	^oF	^oK	in.	cm	in.	cm	Btu/(hr)$(ft^2)(^oF)$	$W/(m^2)(^oK)$	ft^2	m^2	in.	cm	in.	cm	Btu/(hr)$(ft^2)(^oF)$	$W/(m^2)(^oK)$	ft^2	m^2
19	498	532	21	53	9	23	3900	2.20×10^4	4.76	0.44	24	61	15	38	3100	1.76×10^4	7.93	0.74
61	497	531	21	53	8	20	2830	1.60	4.19	.39	24	61	15	38	2670	1.51	7.93	.74
20	494	529	17	43	16	41	3110	1.76	9.69	.90	20	51	19	48	2410	1.37	11.21	1.04
62	493	529	18	46	17	43	2810	1.59	10.20	.95	20	51	19	48	2230	1.26	11.21	1.04
63	450	505	21	53	8	20	3840	2.17	4.19	.39	14	36	13	33	2670	1.51	8.07	.75
64	429	493	22	56	5	13	2735	1.55	2.49	.23	14	36	13	33	2880	1.63	8.07	.75
65	428	493	22	56	6	15	3080	1.74	3.02	.28	14	36	13	37	3340	1.89	8.07	.75
66	438	498	20	51	9	23	3220	1.82	4.85	.45	16	41	15	38	2240	1.27	9.16	.85
67	443	501	22	56	9	23	3380	1.91	4.67	.43	16	41	15	38	2570	1.46	9.16	.85

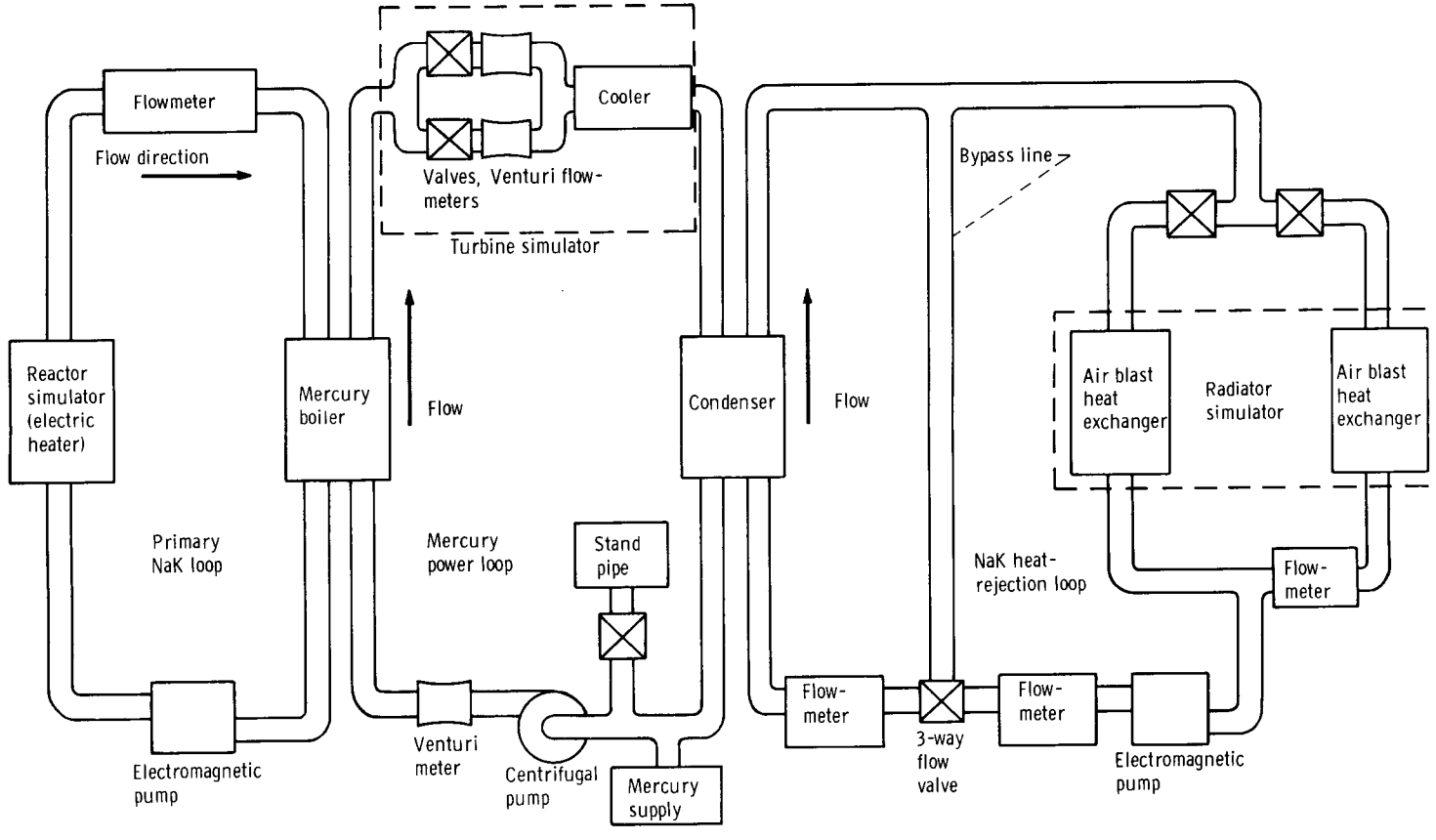

Figure 1. - Simplified schematic of SNAP-8 simulator facility (W-1).

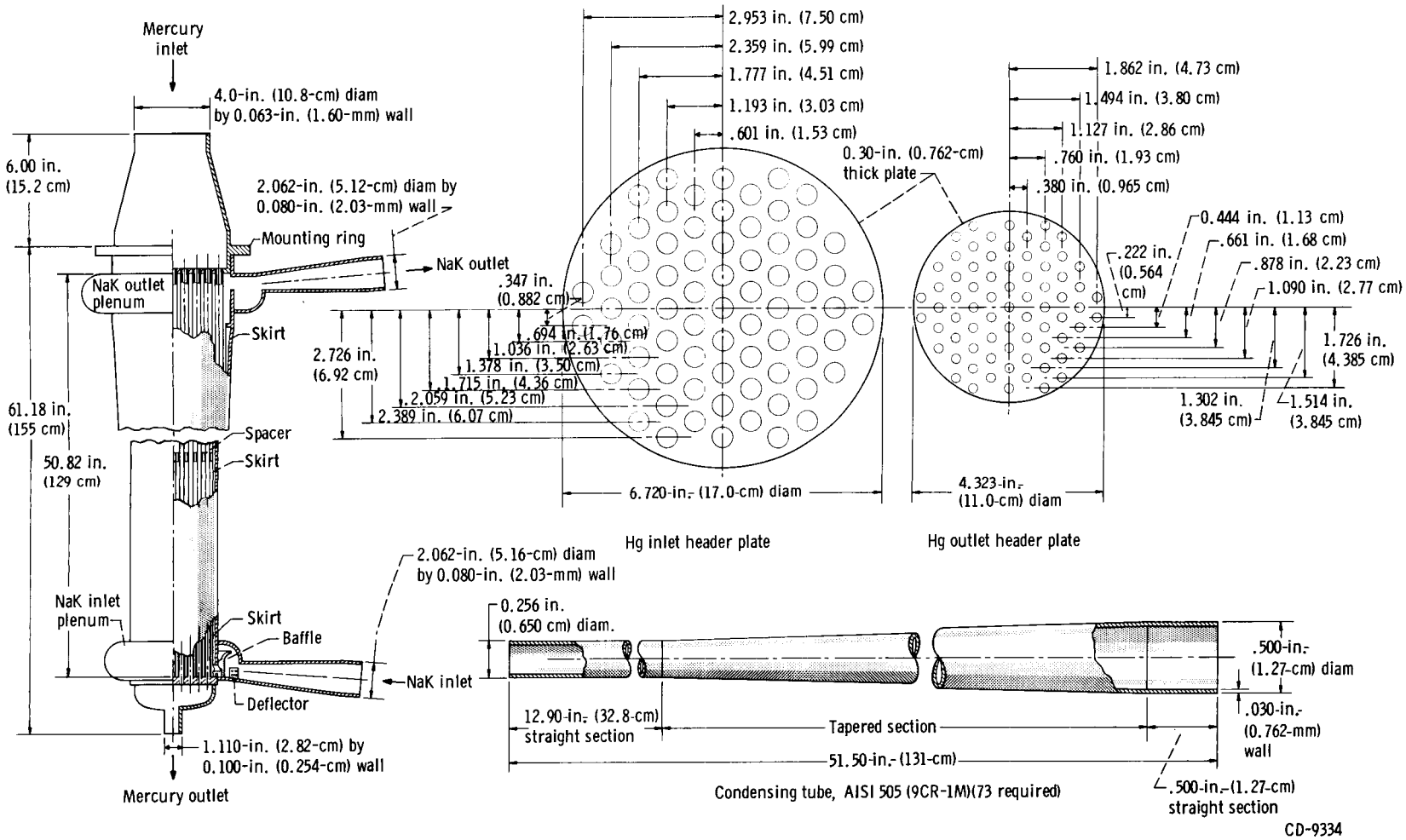

Figure 2. - Mercury condenser.

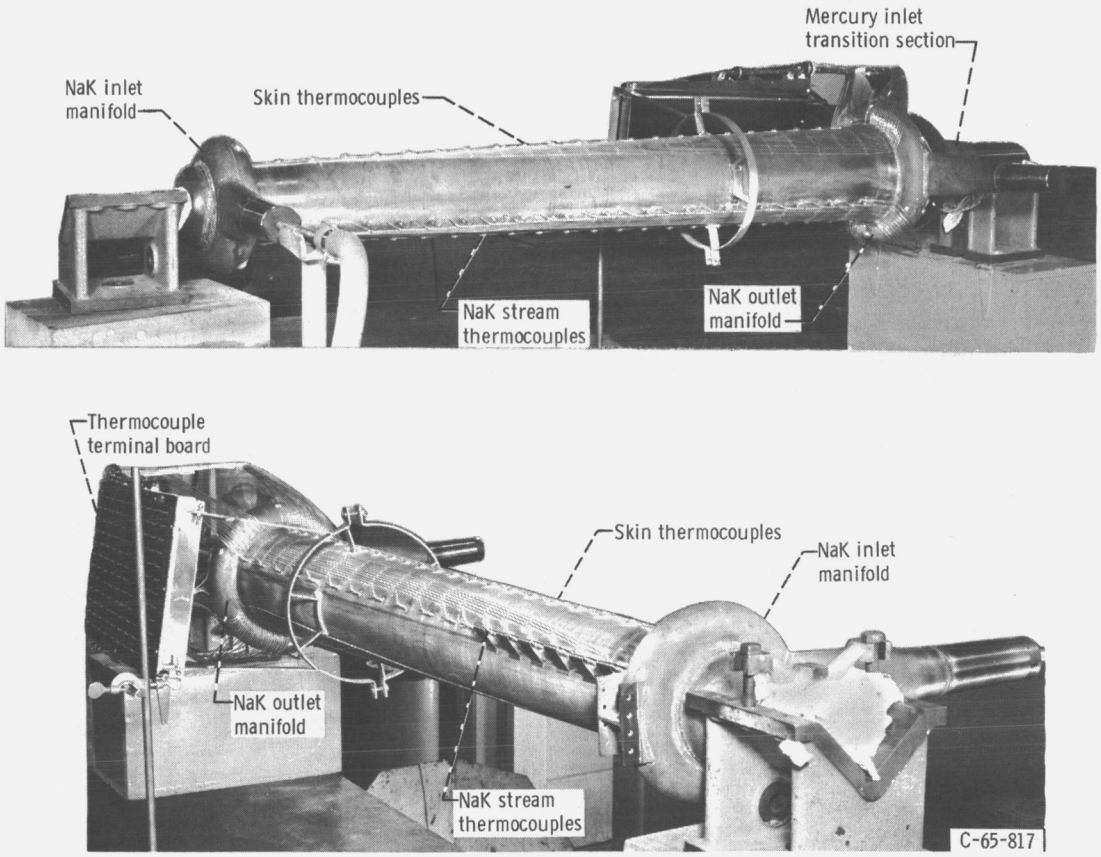

Figure 3. - Instrumented condenser.

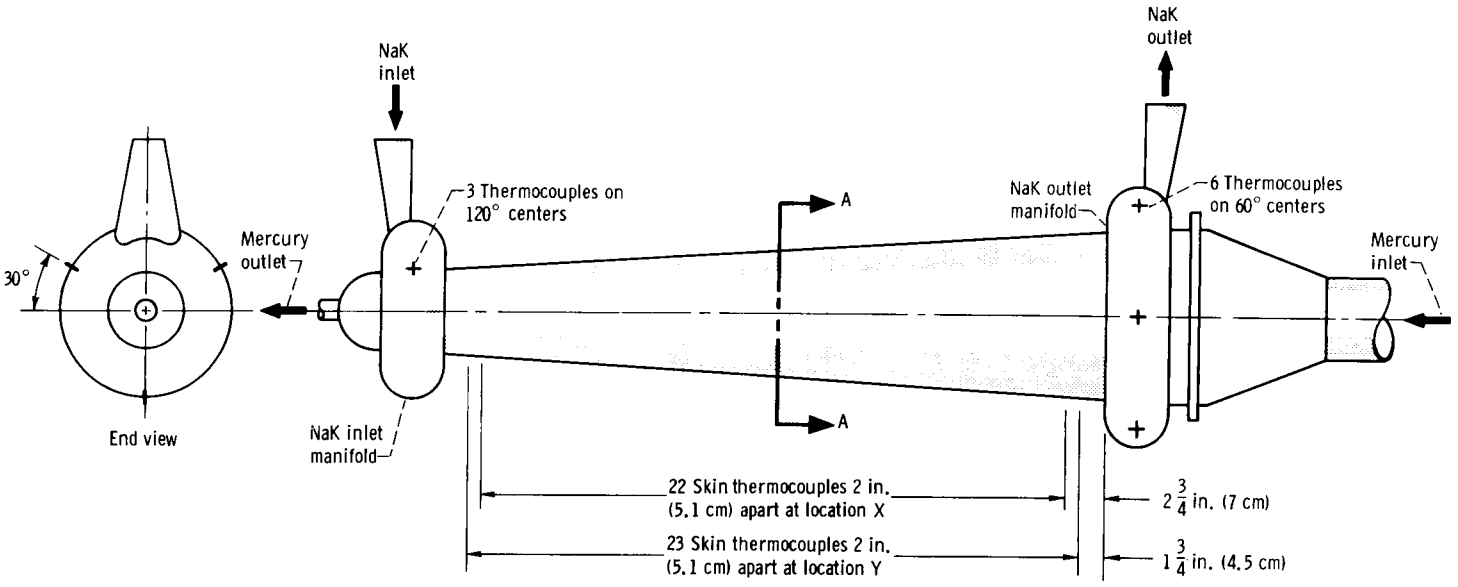

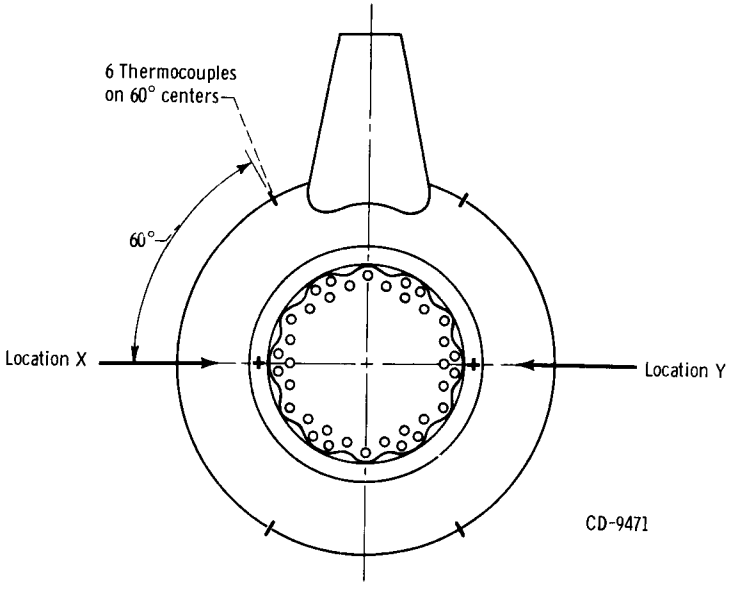

Section A-A

Figure 4. - Condenser assembly showing shell thermocouple locations.

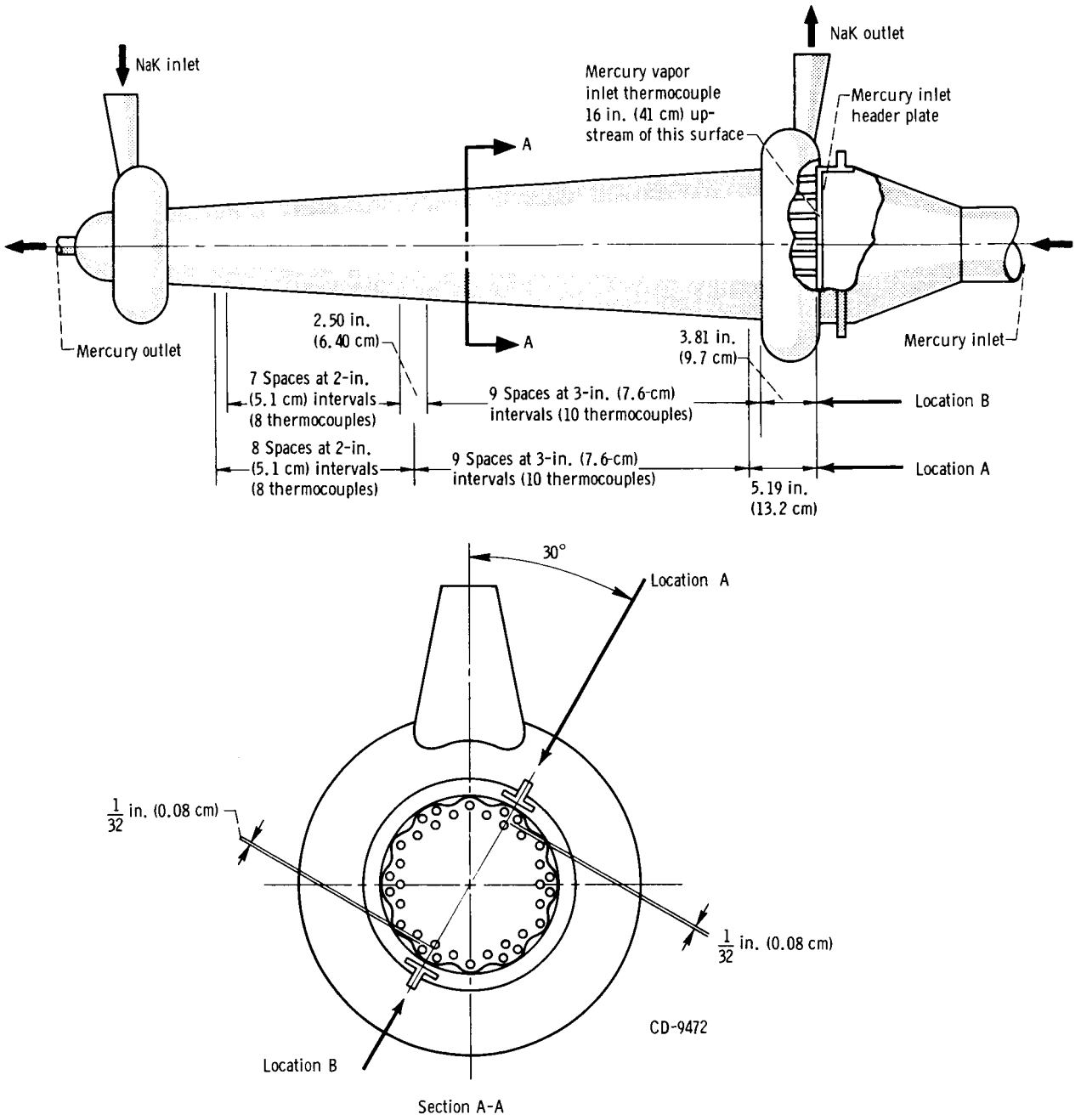

Figure 5. - Condenser assembly cutaway showing immersion thermocouple locations.

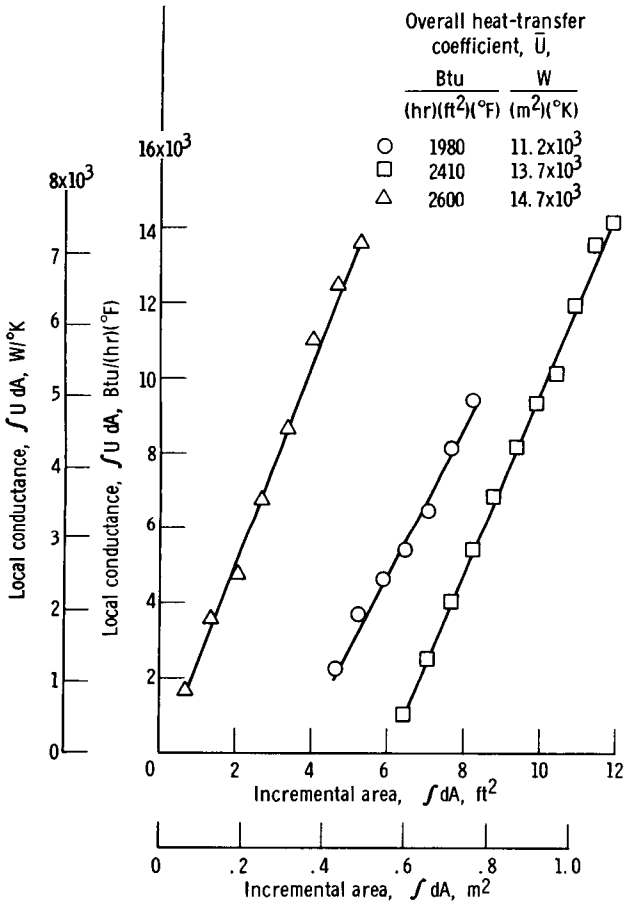

Figure 6. - Typical plot of local conductance as function of incremental area.

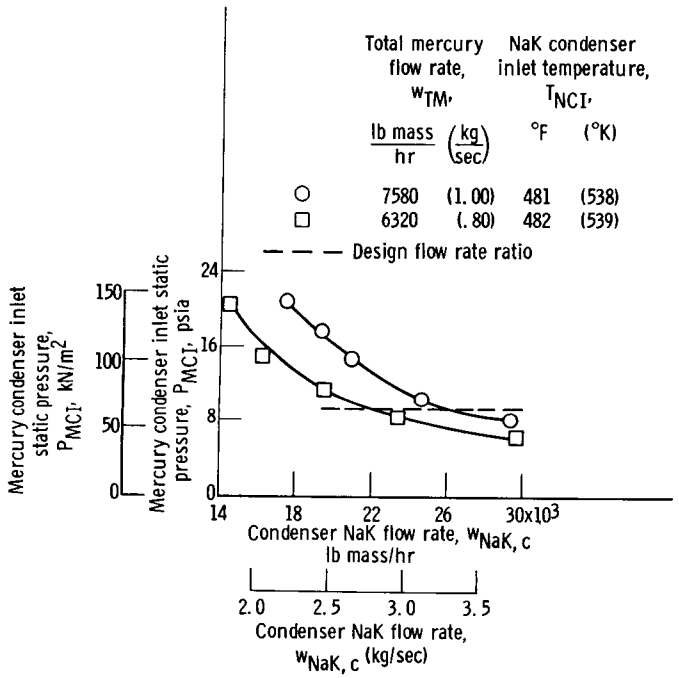

Figure 7. - Mercury condenser inlet static pressure as function of condenser NaK flow rate.

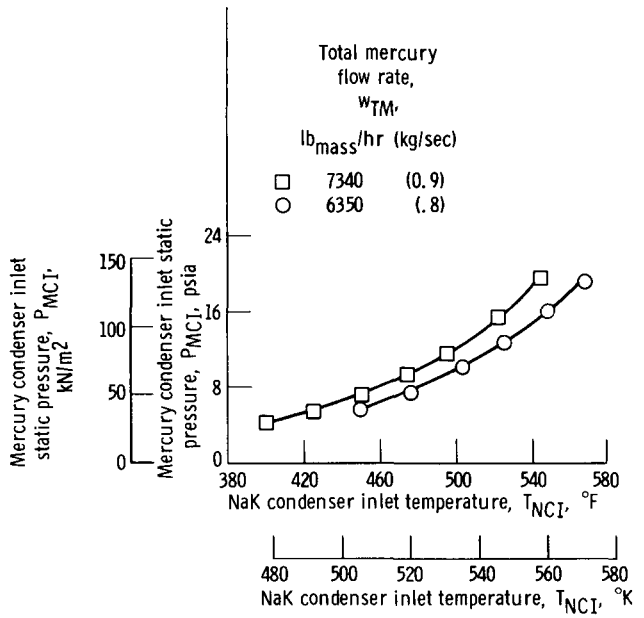

Figure 8. - Mercury condenser inlet static pressure as function of condenser NaK inlet temperature. Flow rate on NaK side of condenser, 29 000 pounds mass per hour (3.7 kg/sec).

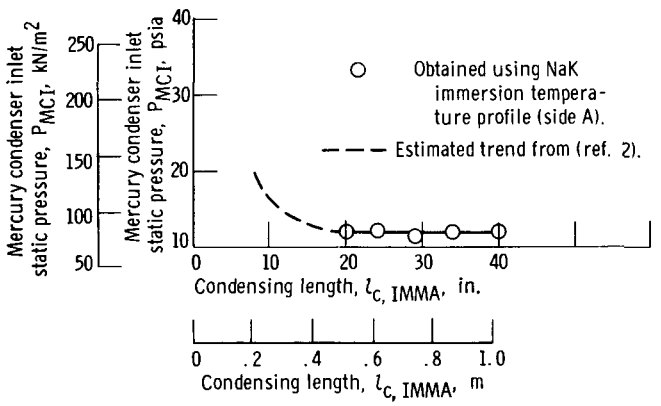

Figure 9. - Mercury condenser inlet static pressure as function of condensing length. Total mercury flow rate, 7440 pounds mass per hour (0.94 kg/sec); NaK condenser inlet temperature, 495° F (530° K).

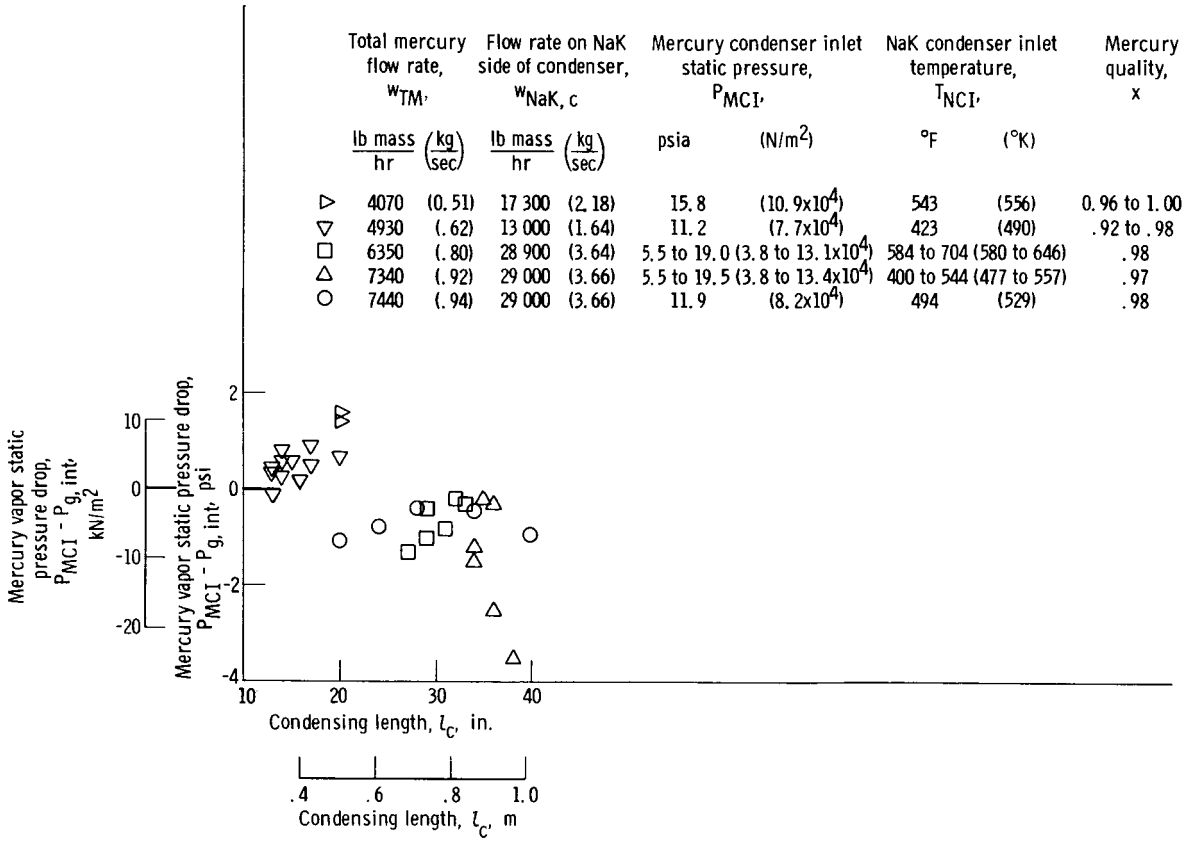

Figure 10. - Experimental mercury vapor static pressure difference as function of condensing length.

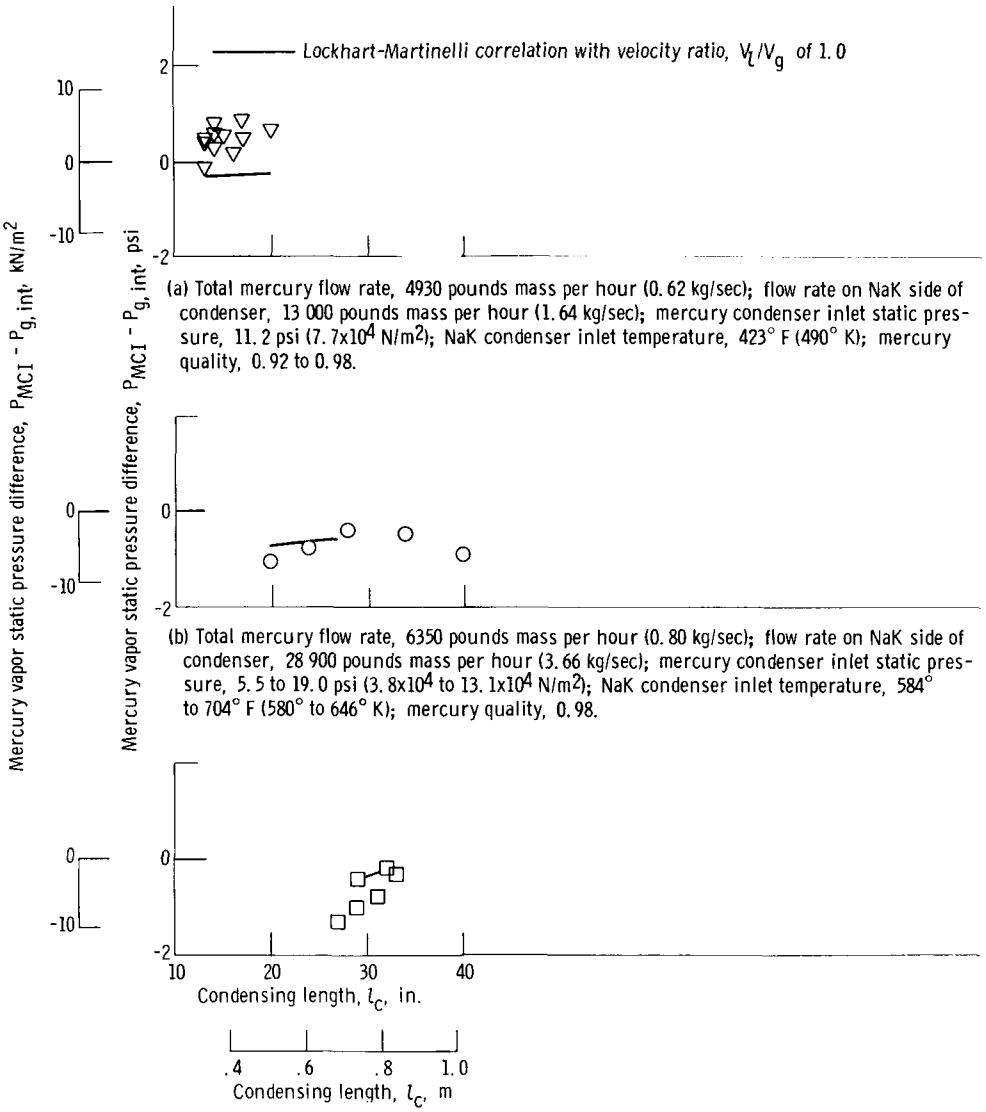

(a) Total mercury flow rate, 4930 pounds mass per hour (0.62 kg/sec); flow rate on NaK side of condenser, 13 000 pounds mass per hour (1.64 kg/sec); mercury condenser inlet static pressure, 11.2 psi (7.7×10^4 N/m^2); NaK condenser inlet temperature, 423° F (490° K); mercury quality, 0.92 to 0.98.

(b) Total mercury flow rate, 6350 pounds mass per hour (0.80 kg/sec); flow rate on NaK side of condenser, 28 900 pounds mass per hour (3.66 kg/sec); mercury condenser inlet static pressure, 5.5 to 19.0 psi (3.8×10^4 to 13.1×10^4 N/m^2); NaK condenser inlet temperature, 584° to 704° F (580° to 646° K); mercury quality, 0.98.

(c) Total mercury flow rate, 7440 pounds mass per hour (0.94 kg/sec); flow rate on NaK side of condenser, 29 000 pounds mass per hour (3.66 kg/sec); mercury condenser inlet static pressure, 11.9 psi (8.2×10^4 N/m^2); NaK condenser inlet temperature, 494° F (529° K) mercury quality, 0.98.

Figure 11. - Comparison of theoretical and experimental pressure drop results.

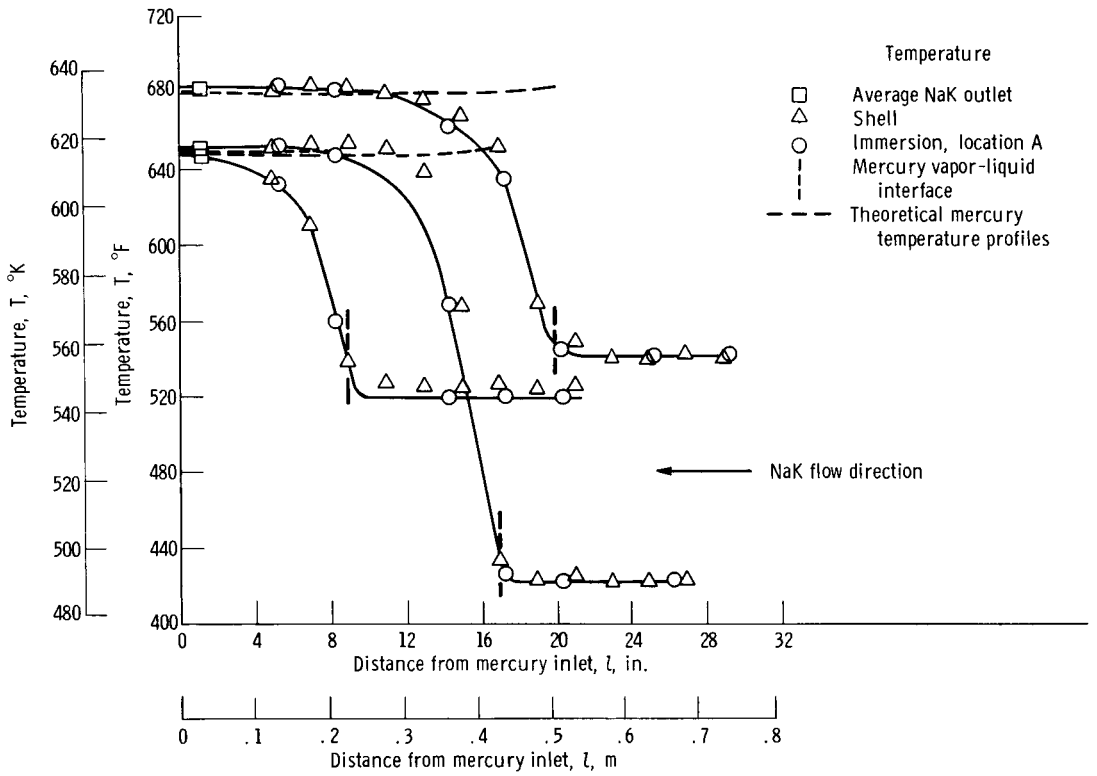

Figure 12. - NaK and theoretical mercury temperature profiles at low NaK flow rates.

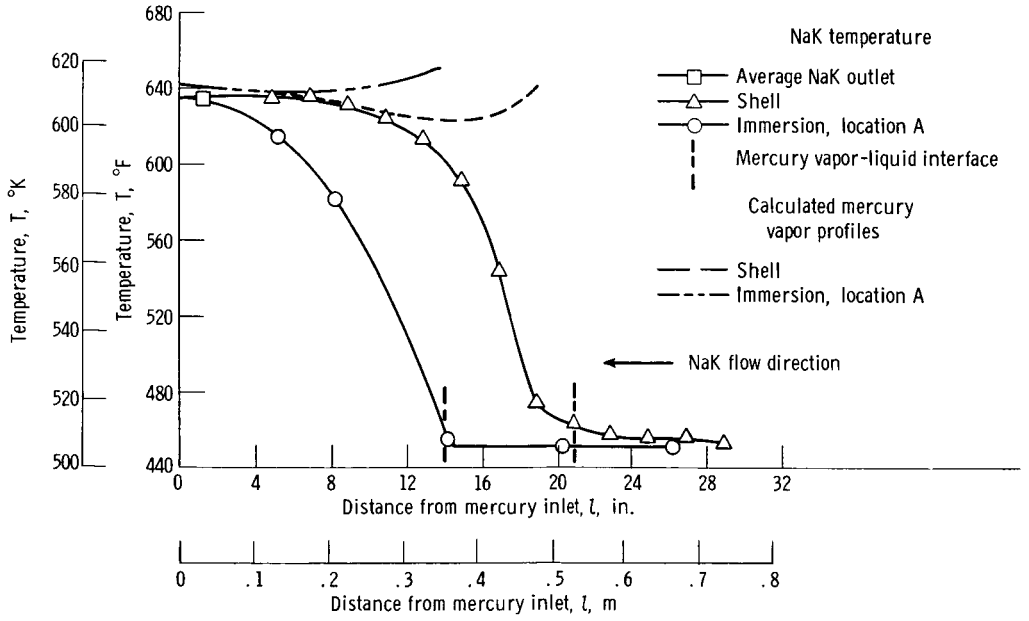

Figure 13. - Temperature profiles from NaK shell thermocouples, NaK immersion thermocouples, and calculated mercury vapor static pressure at high NaK flow rates. Mercury flow rate, 8920 pounds mass per hour (1.12 kg/sec); NaK flow rate, 30 500 pounds mass per hour (3.85 kg/sec).

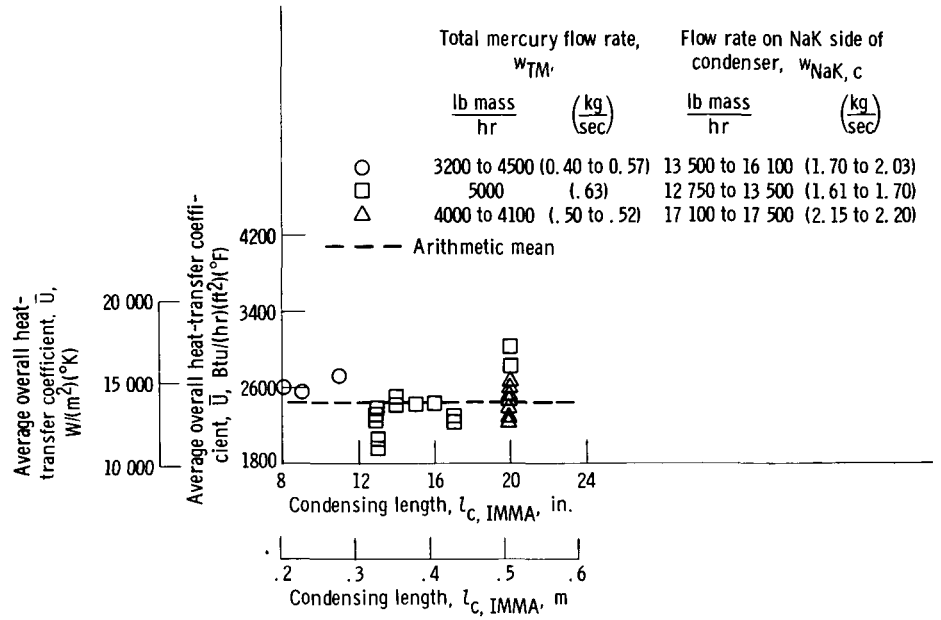

Figure 14. - Average overall condensing heat-transfer coefficient obtained from two-phase static pressure correlation of Lockhart-Martinelli with liquid-to-vapor velocity ratio of 1.0.

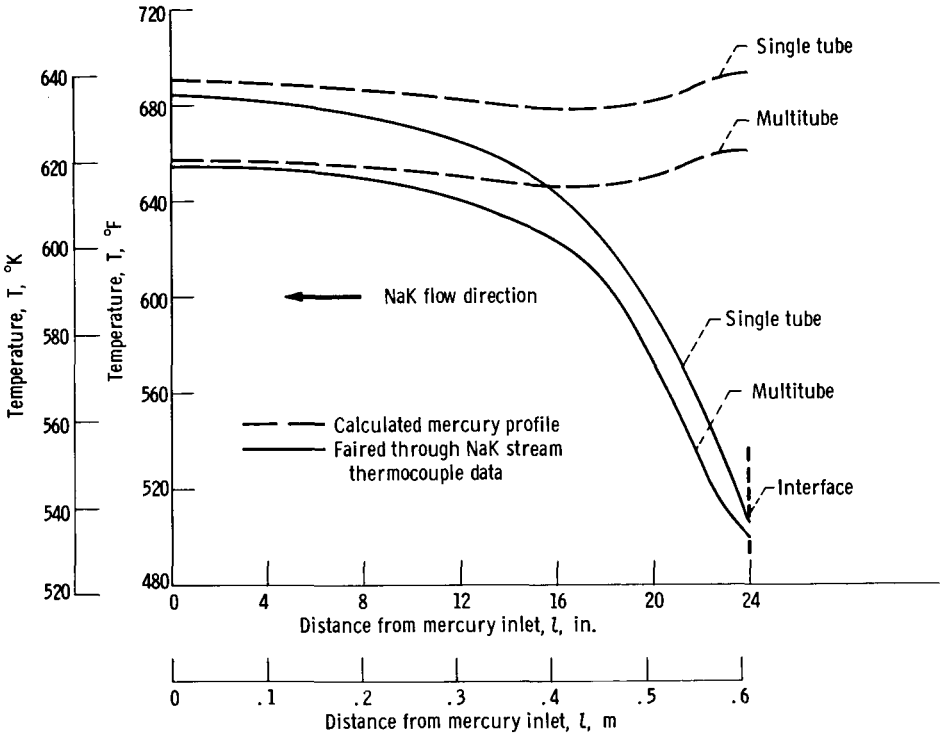

Figure 15. - Measured NaK and calculated mercury temperature profiles for multitube condenser compared with previous single-tube test. Single-tube data (ref. 4): total mercury flow rate, 158 pounds mass per hour (2×10^{-2} kg/sec); flow rate on NaK side of condenser, 513 pounds mass per hour (6.5×10^{-2} kg/sec); immersion thermocouple heat-transfer coefficient, 2880 Btu per hour per square foot per °F (1.63×10^{4} W/(m²)(°K). Multitube condenser data: total mercury flow rate, 7460 pounds mass per hour (0.94 kg/sec) or 102 pounds mass per hour per tube (1.28×10^{-2} kg/sec)/tube); flow rate on NaK side of condenser, 28 980 pounds mass per hour (3.64 kg/sec) or 397 pounds mass per hour per tube (5×10^{-2} (kg/sec)/tube); immersion thermocouple heat-transfer coefficient (location A), 3100 Btu per hour per square foot per °F (1.76×10^{4} W/m²-°K).

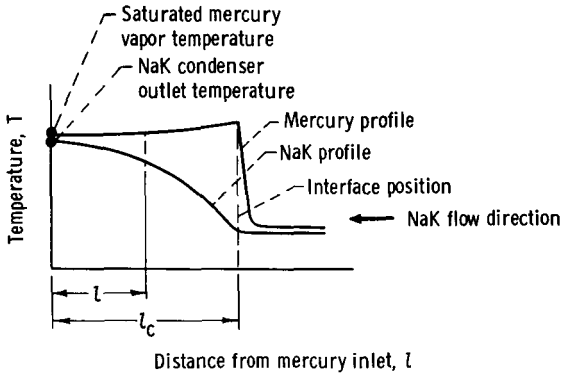

Figure 16. - Temperature of mercury and NaK as function of distance from the mercury inlet.

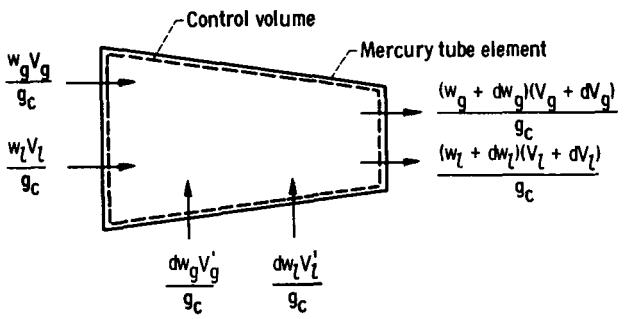

Figure 17. - Liquid and vapor momentum terms.

"The aeronautical and space activities of the United States shall be conducted so as to contribute . . . to the expansion of human knowledge of phenomena in the atmosphere and space. The Administration shall provide for the widest practicable and appropriate dissemination of information concerning its activities and the results thereof."

—NATIONAL AERONAUTICS AND SPACE ACT OF 1958

NASA SCIENTIFIC AND TECHNICAL PUBLICATIONS

TECHNICAL REPORTS: Scientific and technical information considered important, complete, and a lasting contribution to existing knowledge.

TECHNICAL NOTES: Information less broad in scope but nevertheless of importance as a contribution to existing knowledge.

TECHNICAL MEMORANDUMS: Information receiving limited distribution because of preliminary data, security classification, or other reasons.

CONTRACTOR REPORTS: Scientific and technical information generated under a NASA contract or grant and considered an important contribution to existing knowledge.

TECHNICAL TRANSLATIONS: Information published in a foreign language considered to merit NASA distribution in English.

SPECIAL PUBLICATIONS: Information derived from or of value to NASA activities. Publications include conference proceedings, monographs, data compilations, handbooks, sourcebooks, and special bibliographies.

TECHNOLOGY UTILIZATION PUBLICATIONS: Information on technology used by NASA that may be of particular interest in commercial and other non-aerospace applications. Publications include Tech Briefs, Technology Utilization Reports and Notes, and Technology Surveys.

Details on the availability of these publications may be obtained from:

SCIENTIFIC AND TECHNICAL INFORMATION DIVISION

NATIONAL AERONAUTICS AND SPACE ADMINISTRATION

Washington, D.C. 20546